



Research article

Identification of receptors and factors associated with human coronaviruses in the oral cavity using single-cell RNA sequencing

Feng Gao^{a,b,1}, Weiming Lin^{c,1}, Xia Wang^{c,d,1}, Mingfeng Liao^e, Mingxia Zhang^e, Nianhong Qin^f, Xianxiong Chen^a, Lixin Xia^c, Qianming Chen^{g,**}, Ou Sha^{a,b,*}

^a School of Dentistry, Shenzhen University Medical School, Shenzhen University, Shenzhen, China

^b Institute of Dental Research, Shenzhen University, Shenzhen, China

^c Shenzhen University Medical School, Shenzhen University, Shenzhen, China

^d The Chinese University of Hong Kong Shenzhen, School of Medicine, Shenzhen, China

^e The Third People's Hospital of Shenzhen, Shenzhen, China

^f Department of Stomatology, Shenzhen People's Hospital, Shenzhen, China

^g Stomatology Hospital, School of Stomatology, Zhejiang University School of Medicine, Clinical Research Center for Oral Diseases of Zhejiang Province, Key Laboratory of Oral Biomedical Research of Zhejiang Province, Cancer Center of Zhejiang University, Hangzhou, China

ARTICLE INFO

Keywords:

Human coronaviruses
Oral cavity
Proteases
Restriction factors
SARS-CoV-2
scRNA-seq
Viral receptors

ABSTRACT

Severe Acute Respiratory Syndrome Coronavirus-2 (SARS-CoV-2) ravaged the world, and Coronavirus Disease 2019 (COVID-19) exhibited highly prevalent oral symptoms that had significantly impacted the lives of affected patients. However, the involvement of four human coronavirus (HCoVs), namely SARS-CoV-2, SARS-CoV, MERS-CoV, and HCoV-229E, in oral cavity infections remained poorly understood. We integrated single-cell RNA sequencing (scRNA-seq) data of seven human oral tissues through consistent normalization procedure, including minor salivary gland (MSG), parotid gland (PG), tongue, gingiva, buccal, periodontium and pulp. The Seurat, scDblFinder, Harmony, SingleR, Ucell and scCancer packages were comprehensively used for analysis. We identified specific cell clusters and generated expression profiles of SARS-CoV-2 and coronavirus-associated receptors and factors (SCARFs) in seven oral regions, providing direction for predicting the tropism of four HCoVs for oral tissues, as well as for dental clinical treatment. Based on our analysis, it appears that various SCARFs, including ACE2, ASGR1, KREMEN1, DPP4, ANPEP, CD209, CLEC4G/M, TMPRSS family proteins (including TMPRSS2, TMPRSS4, and TMPRSS11A), and FURIN, are expressed at low levels in the oral cavity. Conversely, BSG, CTSB, and CTSL exhibit enrichment in oral tissues. Our study also demonstrates widespread expression of restriction factors, particularly IFITM1-3 and LY6E, in oral cells. Additionally, some replication, assembly, and trafficking factors appear to exhibit broad oral tissues expression patterns. Overall, the oral cavity could potentially serve as a high-risk site for SARS-CoV-2 infection, while displaying a comparatively lower degree of susceptibility towards other HCoVs (including SARS-CoV, MERS-CoV and HCoV-229E). Specifically, MSG, tongue, and gingiva represent potential sites of vulnerability for four HCoVs infection, with the MSG exhibiting a particularly high

* Corresponding author. School of Dentistry, Shenzhen University Medical School, Shenzhen University, Shenzhen, China.

** Corresponding author. Stomatology Hospital, School of Stomatology, Zhejiang University School of Medicine, Clinical Research Center for Oral Diseases of Zhejiang Province, Key Laboratory of Oral Biomedical Research of Zhejiang Province, Cancer Center of Zhejiang University, Hangzhou, China

E-mail addresses: qmchen@zju.edu.cn (Q. Chen), shaou@szu.edu.cn (O. Sha).

¹ These authors contribute equally to this work and share first authorship.

<https://doi.org/10.1016/j.heliyon.2024.e28280>

Received 24 October 2023; Received in revised form 12 March 2024; Accepted 15 March 2024

Available online 16 March 2024

2405-8440/© 2024 The Authors. Published by Elsevier Ltd. This is an open access article under the CC BY-NC license (<http://creativecommons.org/licenses/by-nc/4.0/>).

susceptibility. However, the expression patterns of SCARFs in other oral sites demonstrate relatively intricate and may only be specifically associated with SARS-CoV-2 infection. Our study sheds light on the mechanisms of HCoVs infection in the oral cavity as well as gains insight into the characteristics and distribution of possible HCoVs target cells in oral tissues, providing potential therapeutic targets for HCoVs infection in the oral cavity.

1. Introduction

The emergence of the Severe Acute Respiratory Syndrome Coronavirus-2 (SARS-CoV-2) in 2019 triggered a global pandemic known as Coronavirus Disease 2019 (COVID-19), which can be transmitted through various means including droplets, aerosols, and contact with contaminated surfaces [1–4]. To date, a total of seven distinct human coronaviruses (HCoVs) had been characterized, namely HCoV-229E, HCoV-OC43, SARS-CoV, HCoV-NL63, HCoV-HKU1, Middle East Respiratory Syndrome Coronavirus (MERS-CoV), and SARS-CoV-2 (in chronological order of their emergence). Notably, among these coronaviruses, SARS-CoV, MERS-CoV, and SARS-CoV-2 were recognized as highly pathogenic coronaviruses [5]. The available clinical evidence had established that highly pathogenic coronaviruses shared similar clinical manifestations, and patients typically exhibited symptoms such as fever, chills, cough, myalgia, headache, and dyspnea. Severe cases may progress to acute respiratory distress syndrome (ARDS), resulting in multiple organ dysfunction syndrome (MODS) and even death, primarily among the aged patients with underlying disease [1,6–9]. It was reported that the mortality rates of SARS-CoV, MERS CoV, and SARS-CoV-2 were 9.6%, 34.4%, and 3.5%, respectively [5]. Nonetheless, the remaining four HCoVs (HCoV-NL63, HCoV-229E, HCoV-OC43, and HCoV-HKU1) elicited only mild respiratory tract illness in immunocompetent hosts [5]. With the advancement of the research regarding SARS-CoV-2, the recent investigations reflected that the oral symptoms in COVID-19 patients were the key indicator of viral infection [10,11]. Dysgeusia, xerostomia, and oral mucosal lesions are the three oral symptoms of COVID-19 most frequently observed. There are a number of additional oral symptoms, such as facial paralysis, trigeminal neuralgia, Melkersson-Rosenthal syndrome, macroglossia, anomalies of the temporomandibular joint, pain and swelling of the masticatory muscles, etc., although these secondary symptoms have not been widely documented [10,12–14]. Despite not lethal, oral symptoms can have a substantial impact on a patient's life quality and dental health. Recent evidence indicated that SARS-CoV-2 was detected in the oral cavity, predominantly in squamous epithelium and minor salivary gland (lip), which means that the oral cavity may play a potential role in virus invasion and transmission [15]. Unlike SARS-CoV-2 infection, other HCoVs infection appeared to rarely give rise to oral symptoms. However, it is still unclear whether SARS-CoV-2 and other coronaviruses can actively infect and replicate in the oral cavity, which is crucial to gain further insight into the potential risk of infection in the oral cavity and the oral tropism of coronaviruses [16].

Identifying the oral tropism of coronaviruses necessitates a comprehensive understanding of their cell entry mechanism. The entry of coronaviruses into host cells was predicated upon the interplay between the viral spike (S) protein and host viral receptors, in conjunction with the enzymatic activity that cleaves the S protein, and transpired by means of either cell surface or endosomal entry pathways [17]. SARS-CoV-2, SARS-CoV, and MERS-CoV possessed the capacity to exploit both the cell surface entry and endosomal entry pathways [18,19]. Regardless of the entry pathway employed, angiotensin-converting enzyme 2 (ACE2) served as the primary receptor for both SARS-CoV-2 and SARS-CoV [18,20], while DPP4 acted as the primary receptor for MERS-CoV [21]. Transmembrane serine protease 2 (TMPRSS2) appeared to be one of the major proteases for cleaving S protein for entry via the plasma membrane [18], whereas Cathepsin B (CTSB)/Cathepsin L (CTSL) may perform the priming function during entry through the endosome [22–25]. However, other HCoVs, such as HCoV-229E, HCoV-OC43, and HCoV-HKU1, appeared to demonstrate a greater propensity towards utilizing the cell surface entry pathway [26–28]. HCoV-NL63, on the other hand, employed ACE2 as its primary receptor and primarily enters cells via clathrin-mediated endocytosis [29]. In addition, FURIN appeared to enhance viral infectivity, with the FURIN cleavage motif being identified in SARS-CoV-2, MERS-CoV, HCoV-OC43, and HCoV-HKU1 [17,25,30]. However, previous studies had indicated that ACE2 expression is relatively low in various parts of the oral cavity [31,32]. Additionally, in a study conducted by Hoffmann et al., inhibition of TMPRSS2 using serine protease inhibitors was shown to only partially block SARS-CoV-2 entry into cells [18]. Indeed, Basigin (BSG) had been identified as an alternative receptor for SARS-CoV-2 and SARS-CoV infection [33]. Furthermore, a multitude of proteases such as TMPRSS4/11A [34,35], ADAM10/17 [36] had been established to cleave the S protein of HCoVs. Moreover, the host restriction factors were also prominent modulators limiting virus infection [37]. In addition, certain cellular factors were necessary for virus replication, assembly and trafficking [38]. Thus, considering the widespread oral manifestations of COVID-19 and the intense infectivity of HCoVs, there may be other receptors to mediate the entry or replication process of HCoVs. However, there is currently no comprehensive analysis of entry factors in the oral cavity to evaluate their quantity, proportion, and co-expression in various regions of the oral cavity, as well as to further understand the role played by these factors in SARS-CoV-2 infected oral cavity and SARS-CoV-2 pathogenesis in oral tissues. Further elucidation of viral factors expressed in the oral tissues or cell lines may provide critical insights into predicting infection susceptibility across the oral cavity and inform the development of therapeutic interventions.

Singh et al. profiled 28 SARS-CoV-2 and coronavirus-associated receptors and factors (SCARFs) using single-cell transcriptomics across various healthy human tissues to predict the tropism of human coronaviruses. Based on their research, we conducted an analysis of 45 viral factors relevant to HCoVs to gain a more comprehensive understanding of the viral factors present in various parts of the oral cavity and to investigate the potential for HCoVs to infect oral tissues. These viral factors include 27 genes proposed in Singh et al.'s studies [39], as well as an additional 18 factors that we identified as reliable candidates based on the literature we reviewed (Additional file 1: Table S1). Specifically, we used publicly accessible single-cell RNA sequencing (scRNA-seq) datasets and our previously

published scRNA-seq data through consistent normalization procedures to integrate and compare the expression levels and frequency of SCARFs across different regions in the oral cavity, including minor salivary gland (MSG), parotid gland (PG), tongue, gingiva, buccal, periodontium, and pulp, which are prone to COVID-19 oral symptoms and may be susceptible to HCoVs [40]. The objective of the current research was to gain insight into the types and proportions of cells in oral tissues, the expression levels of SCARFs, and potential HCoVs targets in oral tissues and cells.

2. Methods

2.1. Key resources table

REAGENT or RESOURCE	SOURCE	IDENTIFIER
Software and Algorithms		
Seurat (v4.0.1)	[41]	https://satijalab.org/seurat/
scDblFinder (v1.10.0)	[42]	https://github.com/plger/scDblFinder .
Harmony (v0.1.0)	[43]	https://github.com/immunogenomics/harmony
SingleR (v1.10.0)	[44]	https://github.com/dviraran/SingleR
Ucell (v2.1.2)	[45]	https://github.com/carmonalab/UCell
scCancer (v2.2.1)	[46]	http://lifeome.net/software/scancer/

All analyses of scRNA-seq datasets were performed in R (R version 4.2.2) and significant level was set as 0.05. All significance tests in this paper, unless otherwise stated, were assessed using the two-sided Wilcoxon rank-sum test.

2.2. Buccal tissue

The data obtained from our previously published research was subjected to standardization and normalization through implementation of the Seurat (v4.0.1) package [40]. The scDblFinder (v1.10.0) package was applied to eliminate doublets, and the harmony (v0.1.0) package was utilized to integrate samples and reduce batch effects. Cell clusters annotations were performed through utilization of the singleR (v1.10.0) tool, in conjunction with our own query of marker genes. SCARFs were evaluated using the Ucell (v2.1.2) tool. A comprehensive list of genes and literature sources employed in this research is presented in Additional file 1: [Table S1](#).

2.3. Tongue

We utilized scRNA-seq data from GSE172577 for our analysis in tongue cells. The scCancer package (v2.2.1) was employed with standard procedures and default parameters to perform cell quality control and distinguish between malignant and non-malignant cells. Non-malignant cells identified through this process were then imported into Seurat (v4.0.1) for downstream analysis. The scDblFinder (v1.10.0) package was employed to remove doublets, and the harmony (v0.1.0) package was utilized to integrate samples and mitigate batch effects. Cell cluster annotations were performed using the singleR (v1.10.0) tool, complemented by our own query of marker genes. We evaluated SCARFs using the Ucell (v2.1.2) tool. Detailed information on the genes and literature sources utilized in this study can be found in Additional file 1: [Table S1](#).

2.4. Pulp and periodontium

ScRNA-seq data from GSE161267 for our analysis in pulp and periodontium. The scRNA-seq data underwent standardization and normalization via utilization of the Seurat (v4.0.1) package. The scDblFinder (v1.10.0) package was utilized to eliminate doublets, while cells that exhibited a percentage of mitochondrial genes (percent.mit) exceeding 15.53%, RNA counts (nCount_RNA) falling below 288 or exceeding 8160, as well as number of measured genes (nFeature_RNA) falling below 223 or exceeding 2585 were removed. The batch effects were alleviated through integration of samples using the harmony (v0.1.0) package. Cell cluster annotations were conducted by employing the singleR (v1.10.0) tool, supplemented by our own query of marker genes. The scoring of SCARFs was assessed using the Ucell (v2.1.2) tool. A comprehensive list of genes and literature sources used in this study is provided in Additional file 1: [Table S1](#).

2.5. Parotid gland

For our analysis in parotid gland, we employed scRNA-seq data from GSE188478. We standardized and normalized the scRNA-seq data using the Seurat (v4.0.1) package. The scDblFinder (v1.10.0) package was employed to eradicate doublets, and cells that demonstrated a proportion of mitochondrial genes (percent.mit) exceeding 14.3%, RNA counts (nCount_RNA) less than 535 or greater than 8436, and a measured number of genes (nFeature_RNA) less than 311 or greater than 2108 were excluded from further analysis. Batch effects were mitigated by integrating samples using the harmony (v0.1.0) package. Cell cluster annotations were performed using the singleR (v1.10.0) tool, accompanied by our own inquiry of marker genes. The scoring of SCARFs was evaluated by means of

the Ucell (v2.1.2) tool. A detailed account of the genes and literature sources employed in this study is presented in Additional file 1: [Table S1](#).

2.6. Gingiva and minor salivary gland (MSG)

The scRNA-seq data pertaining to gingival and minor salivary gland from healthy donors was retrieved from the COVID-19 Cell Atlas website [47]. The website had conducted quality control and cell annotation on the data, and we utilized the quality control and annotation results directly in our analysis of scRNA-seq. The scRNA-seq data was transformed into Seurat objects and batch effects were removed by integrating samples using the harmony (v0.1.0) package in R (R version 4.2.2). The assessment of SCARFs was performed utilizing the Ucell (v2.1.2) tool. A comprehensive inventory of the genes and literature sources utilized in the study has been

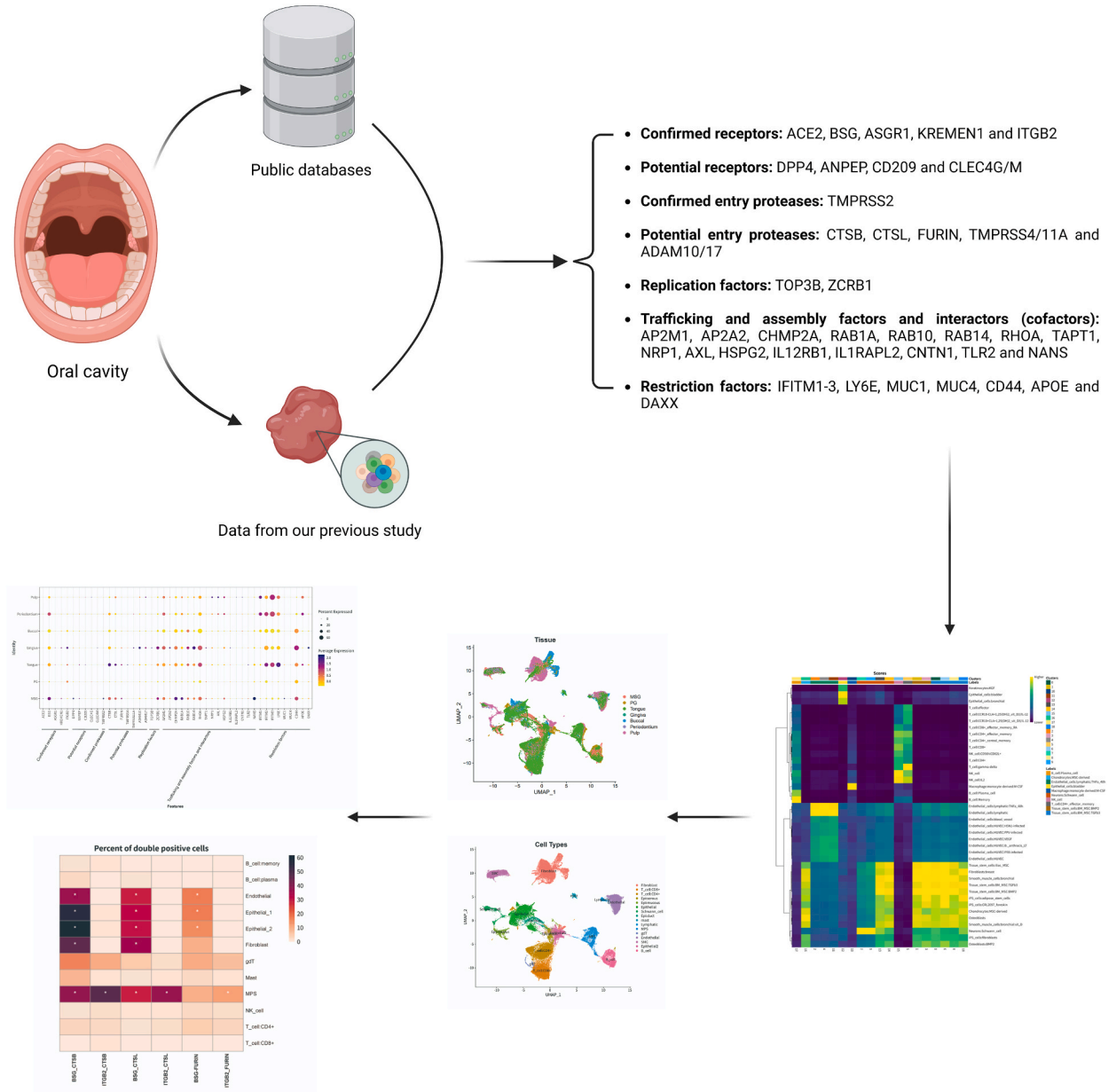


Fig. 1. The analytical process of SCARFs in our research. Our data was acquired from a combination of public databases and prior investigations [40]. Drawing upon previous studies [39] and introducing additional candidates that we deemed trustworthy, we categorized SCARFs into distinct classifications such as confirmed receptors, potential receptors, confirmed entry protease, potential entry protease, replication factors, trafficking and assembly factors and interactors (cofactors), as well as restriction factors. To gain further insight into the expression patterns of SCARFs, we subjected the acquired scRNA-seq data to a clustering analysis based on the markers we queried (figure was created with [Biorender.com](#)).

presented in Additional file 1: Table S1.

2.7. Integration of scRNA-seq data from different sites of oral cavity

The scRNA-seq data from diverse sites of oral cavity were integrated by utilizing the harmony (v0.1.0) package, in order to conduct heterogeneity analysis of cells from distinct parts of oral cavity. SCARFs were scored using the Ucell (v2.1.2) tool. A comprehensive list of the genes and literature sources utilized in the study has been provided in Additional file 1: Table S1.

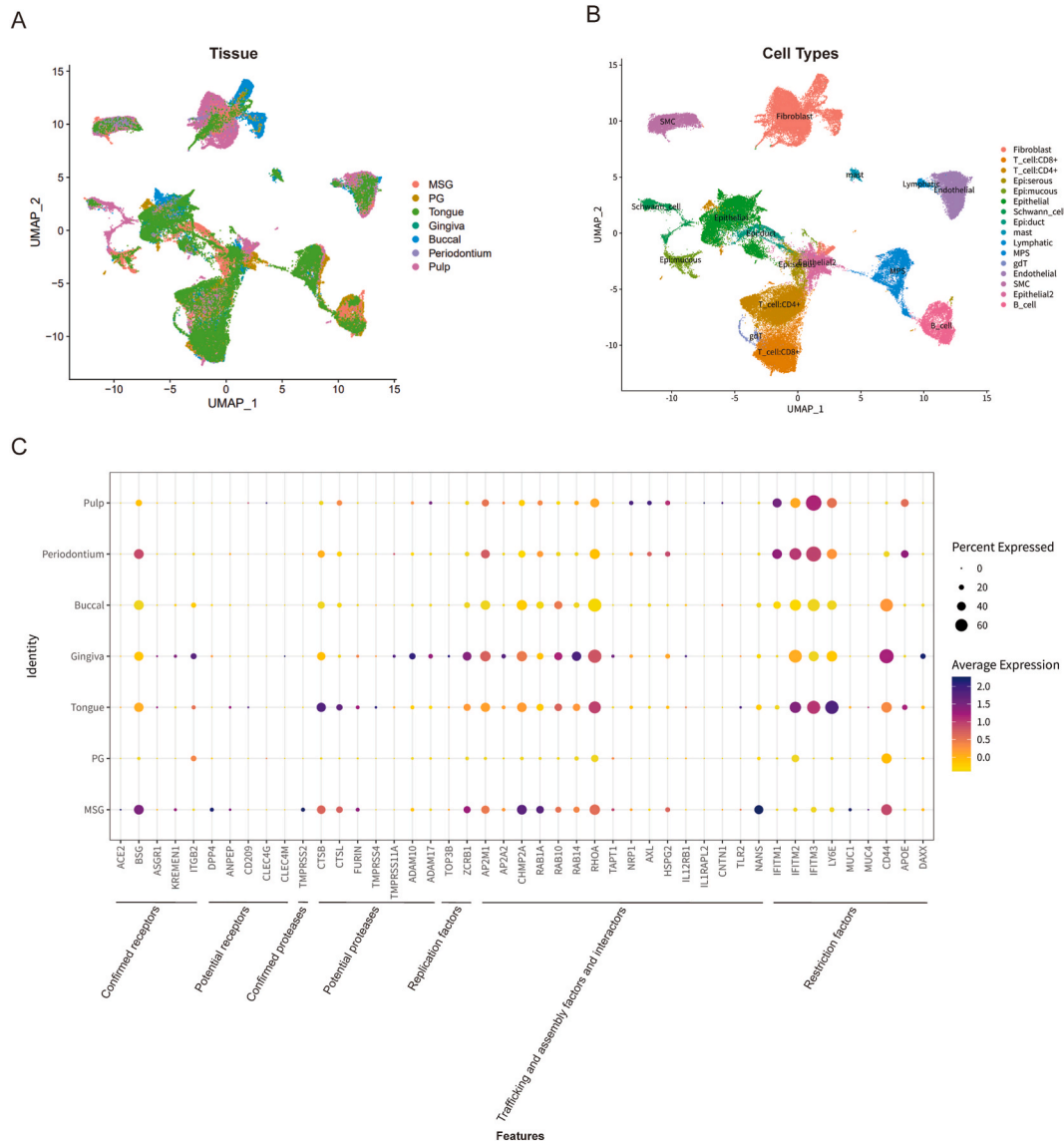


Fig. 2. The scRNA-seq analysis of the expression of SCARFs in oral tissues. **A:** Uniform Manifold Approximation and Projection (UMAP) was used to visualize the clustering of six distinct oral tissue types, including minor salivary glands (MSG), parotid glands (PG), tongue, gingiva, buccal mucosa, periodontium, and pulp. Each cluster is represented by a unique color that corresponds to a specific tissue type. **B:** The cell clusters in the oral cavity are identified by Uniform Manifold Approximation and Projection (UMAP). Cell types identified include fibroblasts, CD8⁺ T cells, CD4⁺ T cells, serous epithelial cells, mucous epithelial cells, epithelial cells, Schwann cells, ductal epithelial cells, mast cells, lymphatic cells, macrophages, gdT cells, endothelial cells, smooth muscle cells, epithelial2 cells, and B cells. Each cluster is represented by a unique color that corresponds to a specific cell type. **C:** Dot plot of gene expression profiles of the 45 SCARFs in each oral tissues. Each dot on the plot reflects the mean expression intensity of the corresponding cell, with yellow and purple denoting low and high expression levels, respectively. The size of each dot varies proportionally with the proportion of cells expressing the SCARFs of interest in the given sample. (For interpretation of the references to color in this figure legend, the reader is referred to the Web version of this article.)

2.8. Calculation of double-positive cells

For each sample, the number of positive cells for a gene was calculated when the count was higher than 0. P value for the percentage of positive cells was estimated using one-sided Fisher's exact test and further adjusted for multiple hypotheses using Bonferroni correction. The percentage of positive cells for a gene in a cell type was compared against the percentage of positive cells for the gene in all the remaining cells. We calculated the overall percentage of positive cells (for a gene or gene pairs) by pooling all the samples together to reduce the effect of drop-out events in scRNA-seq. The code for calculating the number of double-positive cells is available at GitHub website [48].

3. Results

3.1. SCARFs curation

ACE2 and TMPRSS2 were well-established factors known to play a crucial role in facilitating SARS-CoV-2 (as well as SARS-CoV) entry into host cells, but recent research had uncovered additional factors that are essential for the virus's entry and transmission [17]. Below, we listed a series of factors known as SARS-CoV-2 and coronavirus-associated receptors and factors (SCARFs) in previous study [39] that were essential for SARS-CoV-2 as well as other HCoVs infection and transmission (Additional file 1: Table S1). We have enumerated experimentally validated alternative receptors for SARS-CoV-2, such as BSG, ASGR1, KREMEN1, and ITGB2 [33,49,50]. We have additionally enlisted candidate receptors for SARS-CoV-2 that have been previously confirmed for SARS-CoV, MERS-CoV, or HCoV-229E, which include DPP4, ANPEP, CD209, and CLEC4G/M [21,51–53]. Furthermore, our investigation encompassed an examination of several proteases mediating coronavirus entry into host cells, potentially including SARS-CoV-2, such as CTSB, CTSL, FURIN, ADAM10/17, and others [17,22–25,30,36]. We also looked at candidate restriction factors (RFs) that inhibit viral entry through interacting with the HCoVs receptor or the spike protein and limit the replication of HCoVs, which are served as protective mechanisms against HCoVs infection, such as IFITM family proteins (IFITM1-3), Ly6E, mucins (MUC1 and MUC4), CD44, APOE, and DAXX [54–58]. Lastly, we identified factors that may contribute to viral replication, assembly, and trafficking, and that can interact with SARS-CoV-2 protein, such as TOP3B, ZCRB1, AP2 complex (AP2M1 and AP2A2), CHMP2A, Rho-GTPase complex (RAB1A, RAB10, RAB14, and RHOA), TAPT1, NRP1, etc. [38,59,60]. To facilitate analysis, we have categorized the SCARFs related to SARS-CoV-2 into below groups: confirmed receptors, potential receptors, confirmed entry proteases, potential entry proteases, replication factors, trafficking and assembly factors and interactors (cofactors), as well as restriction factors (Fig. 1 and Additional file 1: Table S1). Totally, we enlisted 45 reliable SCARFs seeking to gain insight into the pathogenicity and potential tropism of SARS-CoV-2 in the oral cavity.

3.2. The expression profile of SCARFs in oral cavity

To enhance our understanding of the potential pathogenicity of HCoVs in the oral cavity, we utilized scRNA-seq data from seven human oral tissues to divide them into seven clusters based on the expression levels of specific markers. These clusters include the minor salivary gland (MSG), parotid gland (PG), tongue, gingiva, buccal, periodontium, and pulp. The red dots represent MSG, which is a mucous gland located in the submucosal layer of various regions of the oral cavity, including the labial gland, buccal gland, palatal gland, and lingual gland, mainly composed of acini and ducts. The brown dots represent PG, which is the largest salivary gland in the oral cavity, located below the anterior part of the external auditory canal and on the surface of the posterior part of the masseter muscle. It is mainly composed of acini and ducts. The dark green dots represent the tongue, which is located at the bottom of the oral cavity and can be divided into three parts: the base, the body and the tip. It is composed of the surface mucosa and the deep tongue muscles. The light green dots represent gingiva, which refers to the light red structure that is closely attached to the neck of the tooth and adjacent alveolar bone, composed of multiple layers of flat epithelium and lamina propria. The blue dots represent buccal tissue, which forms the mucosa of the outer wall of the oral vestibule and has barrier function, sensory function, temperature regulation, and secretion function. The purple dots represent periodontal tissue, which refers to the tissue located around the teeth, including alveolar bone, gingiva, and periodontal ligament. The rose red dots represent the pulp, which is located inside the pulp cavity of the tooth and mainly contains nerves, blood vessels, lymph nodes, and connective tissue, as well as odontogenic cells arranged around the pulp (Fig. 2A). Subsequently, we used these scRNA-seq profiles to identify 16 distinct cell clusters within the oral cavity, which consist of five epithelial cell clusters, seven immune cell clusters, and four connective tissue cell clusters (Fig. 2B).

To investigate the oral tissues tropism of HCoVs, we analyzed and compared the expression levels of SCARFs across seven oral tissue types (Fig. 2C). The results showed that ACE2 was expressed only in MSG (0.52%), tongue (0.58%), and gingiva (0.18%). Similarly, TMPRSS2 was expressed in MSG (14.15%), gingiva (0.21%), pulp (0.02%), periodontium (1.50%), and tongue (1.12%), with very low levels in PG and buccal (Fig. 2C and Additional file 2: Table S2). Overall, we observed modest levels of expression of ACE2 and TMPRSS2 across all oral tissues, suggesting that other factors might be involved in the oral tropism of SARS-CoV-2. The expression of other coronavirus receptors, such as DPP4 and ANPEP, was found to be infrequent in oral tissues (Fig. 2C and Additional file 2: Table S2).

Interestingly, our results demonstrated that other potential receptors and proteases such as BSG, ITGB2, CTSB, and CTSL were more extensively expressed (Fig. 2C and Additional file 2: Table S2). FURIN, a protease known to enhance viral tropism and pathogenicity, was moderately expressed in MSG (13.81%) and tongue (13.20%), which may be related to COVID-19 symptoms such as xerostomia and gustatory dysfunction [10,30,61] (Fig. 2C and Additional file 2: Table S2). Nevertheless, the transcription levels of additional

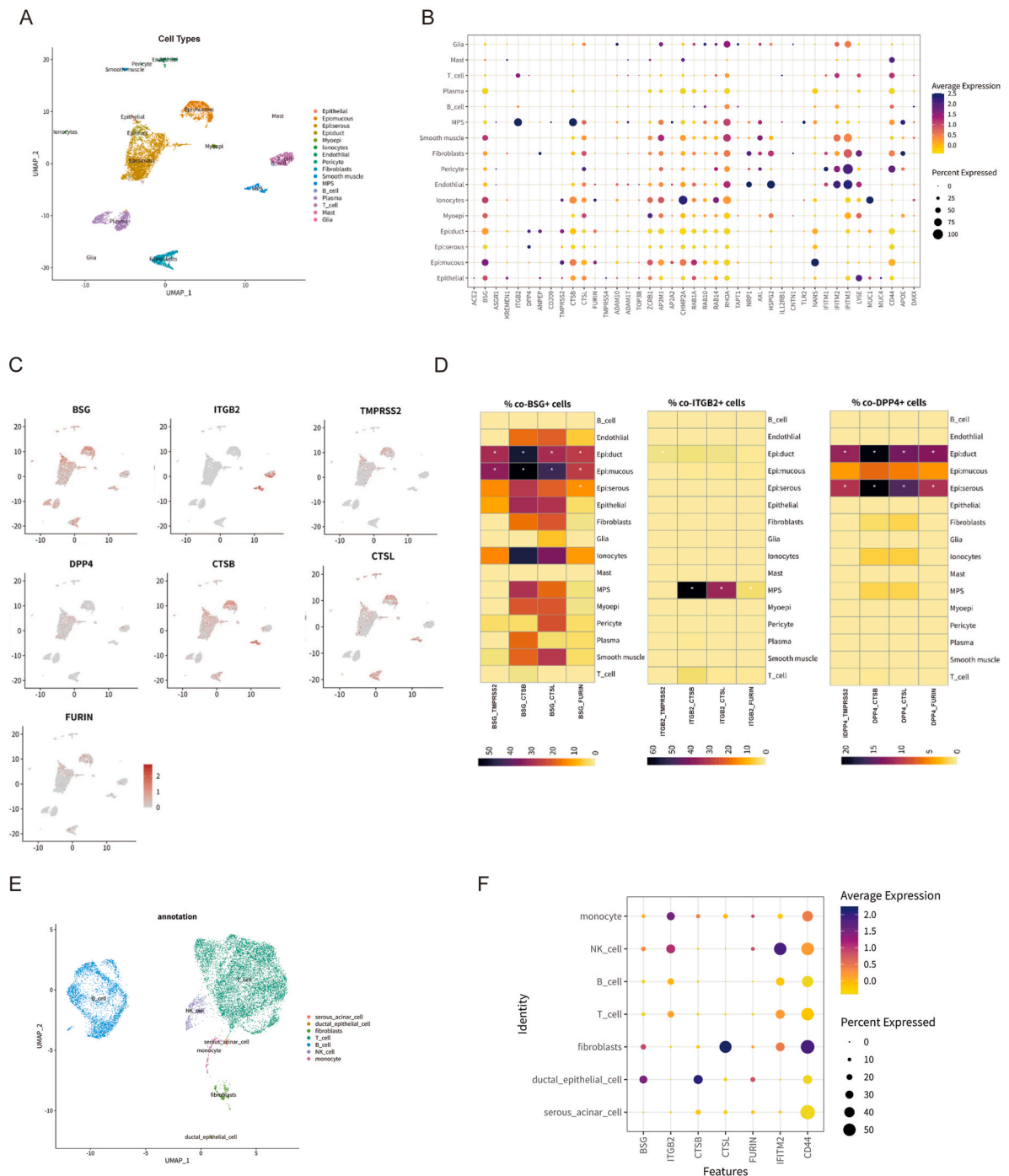


Fig. 3. The scRNA-seq analysis of the expression of SCARFs in MSG and PG. **A:** The UMAP visualization presents specific cell types in the MSG, including epithelial, Epi:mucous, Epi:serous, Epi:duct, myoepi, lonocytes, endothelial, pericyte, fibroblasts, smooth muscle, mononuclear phagocyte system (MPS), B cell, plasma, T cell, mast, and glia. Each color encodes a distinct cell cluster. **B:** The dot plot exhibits the expression levels of SCARFs in specific cell clusters in the MSG. The color of each dot denotes the average expression intensity of the corresponding cell, ranging from low (yellow) to high (purple) expression levels. The size of each dot is proportional to the percentage of cells expressing SCARFs specified in the given sample. **C:** Unsupervised analysis identified cells expressing BSG, ITGB2, DPP4, TMPRSS2, CTSB, CTSL, and FURIN across the MSG's UMAP. Cells are depicted using a color scale that denotes their expression levels, varying from low (grey) to high (red) expression levels. **D:** The heatmap depicts the proportion of double positive cells for different receptor-protease combinations across the 16 specific cell types in the MSG. The color scale represents the expression intensity of each cell type, ranging from low (yellow) to high (dark purple). The stars symbolize the adjusted p value obtained by performing the Fisher's exact test adjusted by the Bonferroni correction. **E:** The UMAP visualization portrays specific cell types in the PG, such as serous acinar cell, ductal epithelial cell, fibroblast, T cell, B cell, NK cell, and monocyte. Each color corresponds to a particular cell type.

F: The dot plot displays the expression levels of COVID-19 genes in specific cell types annotated by marker genes in the PG. The color of each dot indicates the average expression intensity of the corresponding cell, ranging from low (yellow) to high (purple) expression levels. The size of each dot is proportional to the percentage of cells expressing SCARFs specified in the given sample. (For interpretation of the references to color in this figure legend, the reader is referred to the Web version of this article.)

potential proteases, such the TMPRSS family proteins (TMPRSS4 and TMPRSS11A) and the ADAM family proteins (ADAM10 and ADAM17), were limited in oral tissues (Fig. 2C and Additional file 2: Table S2). We also found several factors ZCRB1, AP2A2, CHMP2A, and Rho-GTPase complex (RAB1A, RAB10, RAB14, and RHOA), involved in viral replication, assembly, and trafficking to be expressed in oral tissues, indicating that all oral tissues may potentially assist in viral propagation (Fig. 2C and Additional file 2: Table S2). However, the expression levels of these factors were low in PG (Fig. 2C and Additional file 2: Table S2). The expression of co-factors interacting with SARS-CoV-2 proteins was also modest across most oral tissues, with the exception of NANS, which was highly expressed in MSG (41.28%), suggesting a potentially greater susceptibility to SARS-CoV-2 infection [62] (Fig. 2C and Additional file 2: Table S2). Additionally, our findings indicated that oral tissues express a complex pattern of restriction factors (RFs), with IFITM1-3 and LY6E primarily expressed in pulp, periodontium, buccal, gingiva, and tongue (Fig. 2C and Additional file 2: Table S2). Several RFs, except for CD44, were limitedly expressed in PG and MSG (Fig. 2C and Additional file 2: Table S2). Thus, oral tissues exhibit a complicated pattern of SCARFs expression.

In summary, SCARFs including the receptor, protease, replication, assembly, and trafficking, as well as the cofactor NANS of SARS-CoV-2, were expressed at higher levels in MSG, while restriction factors (except CD44) were expressed at lower levels in MSG. Therefore, MSG exhibited a higher affinity for SARS-CoV-2, and we speculated that it may be one of the main targets of SARS-CoV-2 infection in the oral cavity. Additionally, our findings indicated that oral tissues exhibited low susceptibility to other HCoVs. Moreover, the expression patterns of SCARFs in other tissues, such as pulp, periodontium, buccal, gingiva, and tongue, were more complex, and further investigation was needed to explore the virus's infectivity and replication ability in these tissues. This observation aligned with the infrequent development of parotitis among COVID-19 patients [10].

3.3. Minor salivary gland and parotid gland

3.3.1. Minor salivary gland (MSG)

We analyzed the scRNA-seq datasets for MSG derived from healthy donors collected by COVID-19 Cell Atlas website [47], and 16 cell types were identified. These cell types included epithelial, mucous epithelial cell (Epi:mucous), serous epithelial cell (Epi:serous), ductal epithelial cell (Epi:duct) and myoepi, all of which belong to the epithelial compartment. Additionally, ionocytes, which were first discovered in the lung by Montoro and Plasschaert et al., were found in MSG and may play a role in maintaining physiological saliva ion homeostasis [63,64]. Endothelial, pericyte, fibroblasts, smooth muscle, and glia cells were identified in the connective tissue compartment, although these appeared to be only a small fraction of MSG. Five distinct populations of immune cells were identified, including the mononuclear phagocyte system (MPS), B cell, plasma, T cell and mast cells (Fig. 3A). These findings indicated the intricate composition of MSG.

We found that ACE2 and TMPRSS2 were mainly detected in epithelial, mucous epithelial cell, serous epithelial cell and ductal epithelial cell (Fig. 3B and C and Additional file 3: Table S3), consistent with the research by Huang et al. [16]. However, low-frequency co-expression of ACE2 and TMPRSS2 was observed in epithelial clusters, leading us to investigate the expression of alternative/putative receptors and potential proteases among the 16 MSG cell types (Fig. 3A–C and Additional file 3: Table S3). Dot plot and uniform manifold approximation and projections (UMAPs) of SCARFs expression indicated that BSG, CTSS and CTSL exhibited extensive expression patterns across MSG cells. However, the expression levels of other alternative/putative receptors and potential proteases, including ASGR1, KREMEN1, DPP4, ANPEP, CD209, FURIN, TMPRSS4, ADAM10 and ADAM17, are relatively lower. ITGB2, also known as lymphocyte function-associated antigen 1 (LFA-1), displayed tissue-specific expression patterns and was enriched in immune cells, with the highest expression in MPS (Fig. 3B and C and Additional file 3: Table S3). Interestingly, the receptors and proteases mentioned above were generally expressed at low levels in B cells, T cells, plasma, mast, and glia (Fig. 3B and C and Additional file 3: Table S3). Additionally, most MSG cells expressed some amount of replication, assembly, and trafficking factors as well as cofactors, indicating their potential contribution to viral replication, assembly, and trafficking and to promoting viral infection by cofactors (Fig. 3B and Additional file 3: Table S3). We observed that most MSG cells, except for B cells, T cells, mast cells, and glia, co-expressed receptors and proteases, particularly mucous epithelial cell, serous epithelial cell and ductal epithelial cell. Furthermore, BSG⁺CTSS⁺ cells and BSG⁺CTSL⁺ cells were the predominant double-positive cells, likely due to the relatively higher expression levels of BSG, CTSS, and CTSL in MSG cells. Notably, only MPS exhibited significant ITGB⁺CTSS⁺, ITGB2⁺CTSL⁺, and ITGB2⁺FURIN⁺, possibly ascribed to ITGB2 tissue-specific expression in immune cells (Fig. 3D).

Our study suggested that epithelial cells in MSG, especially mucous epithelial cell, serous epithelial cell, ductal epithelial cell and MPS, have a higher potential risk of SARS-CoV-2 infection. As the main function of MSG epithelial cells is to secrete and excrete saliva, damage to these epithelial cells may lead to saliva secretion and excretion disorders, which may explain the high incidence of xerostomia in COVID-19 patients [10,14,16,65].

3.3.2. Parotid gland (PG)

We further analyzed the expression levels of SCARFs in the parotid gland (PG). The PG was annotated into 7 cell clusters including 4 immune cell clusters, 1 connective tissue cell cluster and 2 epithelial cell clusters (Fig. 3E). Most SCARFs, including ACE2, DPP4,

ANPEP, CD209, CLEL4G/M and TMPRSS family proteins (TMPRSS2, TMPRSS4, and TMPRSS11A), were weakly expressed in PG (Fig. 2C and Additional file 2: Table S2). Therefore, we selected several highly expressed and representative factors for analysis, including BSG, ITGB2, CTSB, CTSL, FURIN, IFITM2 and CD44 (Fig. 3F). The results suggested that ductal epithelial cells exhibited the highest BSG expression, followed by fibroblasts (Fig. 3F and Additional file 4: Table S4). The expression of ITGB2 confined primarily to immune cell populations including T cell (24.20%), B cell (23.50%), NK cell (34.36%) and monocyte (30.43%) (Fig. 3F and Additional file 4: Table S4). Furthermore, CTSB and FURIN showed the highest expression in ductal epithelial cells, while CTSL expression was remarkably higher in fibroblasts (Fig. 3F and Additional file 4: Table S4). Additionally, the restriction factor IFITM2 was enriched in fibroblast and immune cell clusters, and CD44 was widely expressed in PG cells (Fig. 3F and Additional file 4: Table S4). Taken together, it appears that the majority of factors are expressed at low levels in the PG.

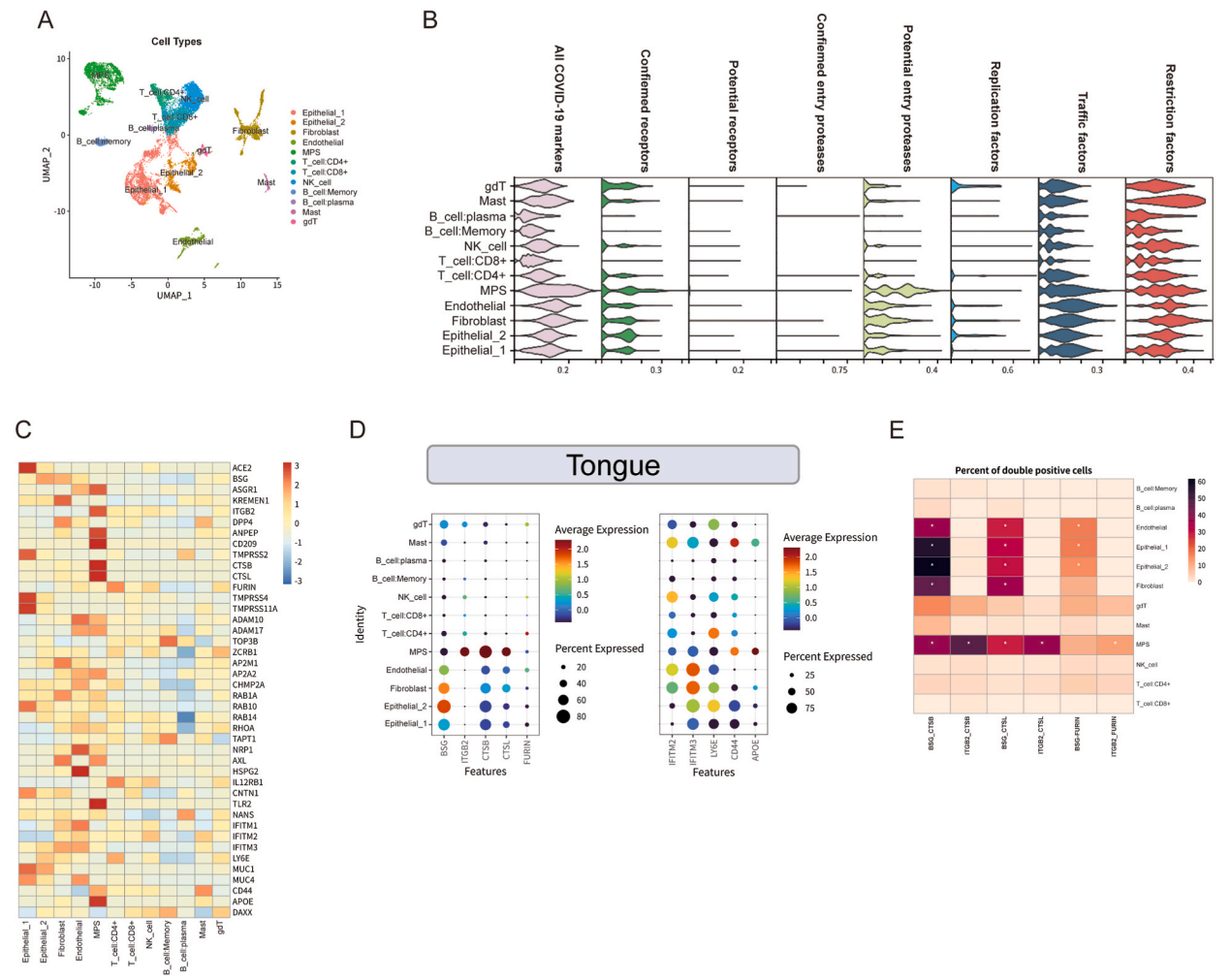


Fig. 4. The scRNA-seq analysis of the expression of SCARFs in tongue. **A:** The UMAP exhibits the specific cell clusters in the tongue, including Epithelial, epithelial2, fibroblast, endothelial, MPS, T cell:CD4⁺, T cell:CD8⁺, NK cell, B cell:Memory, B cell:plasma, mast, and gdT. Each color encodes a distinct cell cluster. **B:** The violin plot displays the expression levels of SCARFs in specific cell types of the tongue. Each color corresponds to a particular SCARFs type. **C:** The presented heatmap showcases transcript levels of SCARFs across specific cell clusters in the tongue. The color gradient spans from blue to red, signifying low to high transcript levels. **D:** The dot plot illustrates the expression of SCARFs in specific cell types annotated in the tongue. The color of each dot indicates the average expression intensity of the corresponding cell, ranging from low (dark blue) to high (Deep red) expression levels. The size of each dot is proportional to the percentage of cells expressing SCARFs specified in the given sample. **E:** The heatmap depicts the proportion of double positive cells for different receptor-protease combinations across the 12 specific cell clusters in the tongue. The color scale ranges from light yellow to deep purple, corresponding to low to high proportions of double positive cells. The stars denote the adjusted p value obtained by the Fisher's exact test adjusted by the Bonferroni correction, indicating the statistical significance of the observed differences between the cell populations. (For interpretation of the references to color in this figure legend, the reader is referred to the Web version of this article.)

3.4. Tongue

UMAPs demonstrated distinct clusters of tongue, including epithelial cell (epithelial_1 and epithelial_2), fibroblast, endothelial, MPS, CD4⁺ T cell, CD8⁺ T cell, NK cell, Memory B cell, plasma, mast and gdT (Fig. 4A).

The visualized expression maps for SCARFs showed that the receptors and proteases as well as replication, assembly and transport factors were primarily distributed in epithelial_1, epithelial_2, fibroblast, endothelial and MPS clusters (Fig. 4B–D). Normalized expression matrices for SCARFs demonstrated that ACE2 and TMPRSS family proteins (TMPRSS2, TMPRSS4 and TMPRSS11A) were

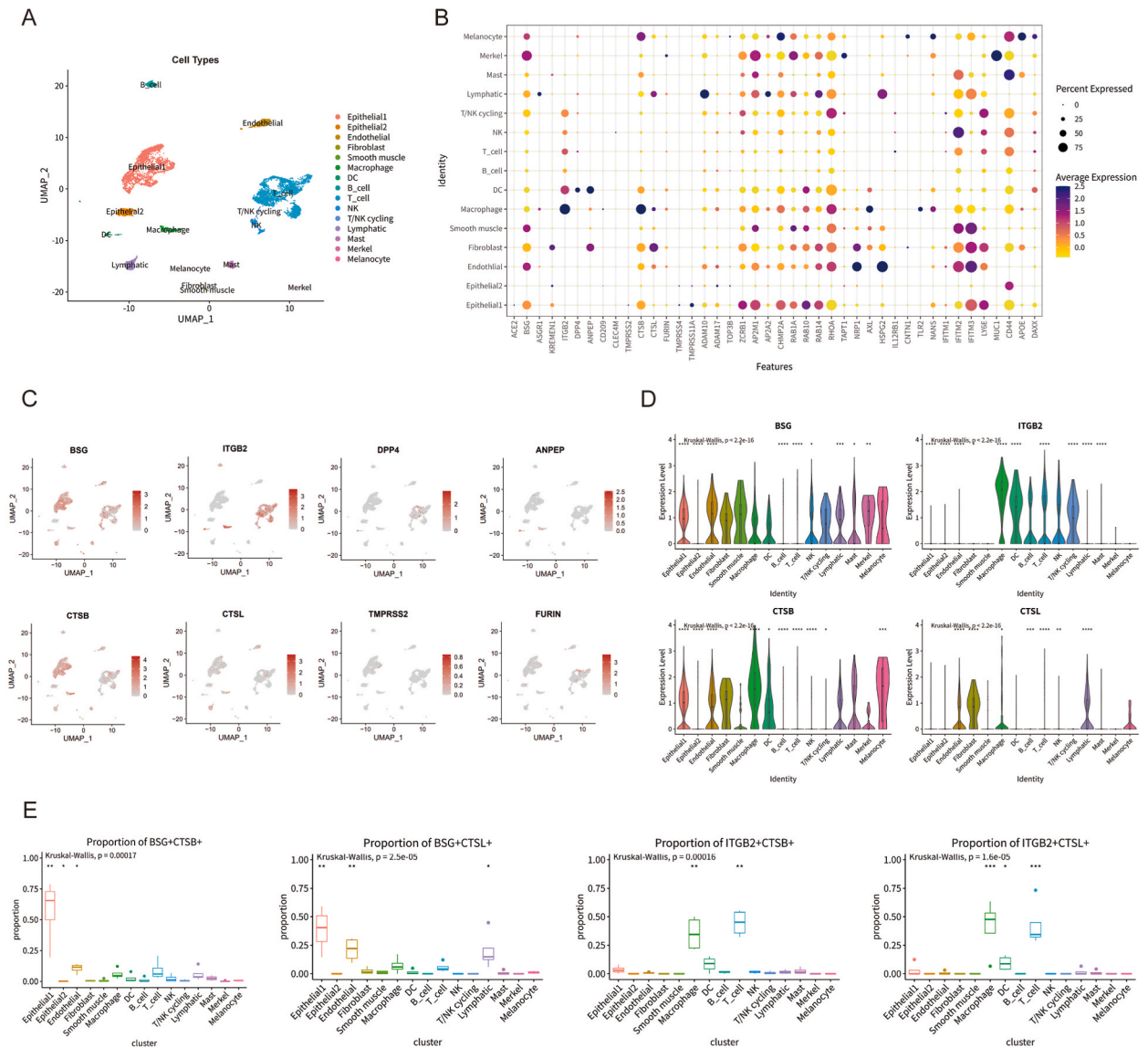


Fig. 5. The scRNA-seq analysis of the expression of SCARFs in gingiva. **A:** The UMAP exhibits the specific cell clusters in the gingiva, including epithelial, epithelial2, endothelial, fibroblast, smooth muscle, macrophage, dendritic cells (DC), B cell, T cell, NK cell, T/NK cycling, lymphatic, mast, Merkel and melanocyte. Each color encodes a distinct cell cluster. **B:** The dot plot illustrates the expression of SCARFs in specific cell types annotated in the gingiva. Each dot on the plot reflects the mean expression intensity of the corresponding cell, with yellow and purple denoting low and high expression levels, respectively. The size of each dot varies proportionally with the proportion of cells expressing the SCARFs of interest in the given sample. **C:** Unsupervised identification of cells expressing BSG, DPP4, ANPEP, CTSS, CTSL, TMPRSS2 and FURIN across the tongue's UMAP. Cells are colored according to their expression levels, ranging from grey (low expression) to red (high expression). **D:** Violin plot showing BSG, ITGB2, CTSS and CTSL expression in 15 specific cell clusters in gingiva. Each color encodes a distinct cell cluster. Stars represent the adjusted p value obtained by Kruskal-Wallis test. **E:** Boxplots illustrating the percentages of BSG⁺CTSS⁺, BSG⁺CTSL⁺, ITGB2⁺CTSS⁺ and ITGB2⁺CTSL⁺ cells in 15 specific cell clusters in the gingiva. Stars represent the adjusted p value obtained by Kruskal-Wallis test. (For interpretation of the references to color in this figure legend, the reader is referred to the Web version of this article.)

highly enriched in epithelial clusters (Fig. 4C). The fibroblast cell clusters exhibited the highest levels of DPP4 expression, while MPS cell clusters demonstrated a noticeable expression of ANPEP. Moreover, we validated that BSG was broadly expressed in tongue cell clusters, particularly in epithelial_2 (80.76%) and epithelial_1 (68.92%), while proteases CTSB and CTSL expression were evident across epithelial_1, epithelial_2, fibroblast, endothelial and MPS (Fig. 4C and D and Additional file 5: Table S5). Additionally, RFs were broadly expressed in tongue cell clusters at significant transcript levels (Fig. 4B–D and Additional file 6: Table S6).

To more precisely characterize the permissiveness of different tongue cell clusters to SARS-CoV-2 infection, we analyzed the co-expression of alternative receptor-potential proteases in 12 cell clusters, including BSG-CTSB, BSG-CTSL, BSG-FURIN, ITGB2-CTSB, ITGB2-CTSL and ITGB2-FURIN. Our analysis showed that BSG-CTSB had a high percentage of double-positive expression in epithelial_1, epithelial_2, fibroblast, endothelial and MPS (35.8%–61.7%), the same pattern applies to BSG-CTSL (28.4%–35.3%). ITGB2-CTSB was proportionally higher in MPS cells (47.0%), the same pattern applies to ITGB2-CTSL (36.7%) (Fig. 4E and Additional file 7: Table S7).

Our results showed that epithelial_1, epithelial_2, fibroblast, endothelial, and MPS cell clusters had been identified as potentially highly susceptible to SARS-CoV-2 infection. Additionally, fibroblast cell clusters may exhibit a heightened vulnerability to MERS-CoV infection, while MPS cell clusters may be particularly susceptible to HCoV-229E infection.

3.5. Gingiva

Using published scRNA-seq datasets from COVID-19 Cell Atlas website [47], we generated an UMAP for 15 cell clusters in gingiva: epithelial 1, epithelial2, endothelial, fibroblast, smooth muscle, macrophage, dendritic cell (DC), B cell, T cell, NK cell, T/NK cycling, lymphatic, mast cell, Merkel and melanocyte (Fig. 5A).

Our analysis of SCARFs expression identified that ACE2 and TMPRSS2 were only expressed in epithelial1 clusters, weakly, which was accordant with Huang et al. [16] (Fig. 5B and Additional file 8: Table S8). BSG was generally detected in gingiva cell populations, while ITGB2 enriched in immune cells, especially in macrophage (Fig. 5B–D and Additional file 8: Table S8). Moreover, the expression

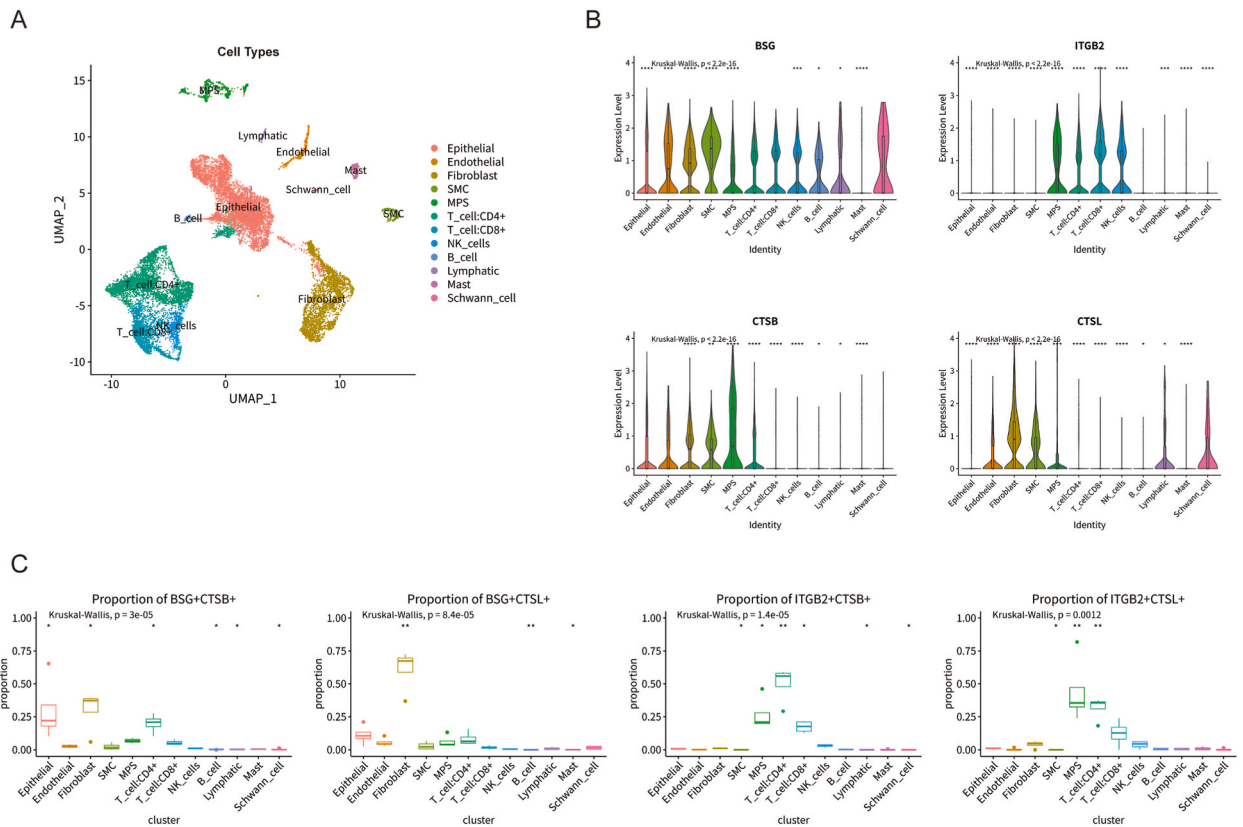


Fig. 6. The scRNA-seq analysis of the expression of SCARFs in buccal tissue. **A:** The UMAP visualization portrays specific cell types in the buccal, including epithelial, endothelial, fibroblast, smooth muscle cell, MPS, T cell:CD4⁺, T cell:CD8⁺, NK cells, B cell, lymphatic, mast, Schwann cell. Each color encodes a distinct cell cluster. **B:** Violin plot showing BSG, ITGB2, CTSB and CTSL expression in 12 specific cell clusters in the buccal. Each color encodes a distinct cell cluster. Stars represent the adjusted p value obtained by Kruskal-Wallis test. **C:** Boxplots illustrating the percentages of BSG⁺CTSB⁺, BSG⁺CTSL⁺, ITGB2⁺CTSB⁺ and ITGB2⁺CTSL⁺ cells in 12 in specific cell clusters in the buccal. Stars represent the adjusted p value obtained by Kruskal-Wallis test. (For interpretation of the references to color in this figure legend, the reader is referred to the Web version of this article.)

approximately 75%. Moreover, ITGB2⁺CTSB⁺ cells and ITGB2⁺CTSL⁺ cells were evident in macrophage and T cell populations (Fig. 5E).

In summary, our results indicated that gingival harbored potent defense mechanisms against HCoV infection. However, it was plausible that epithelial, endothelial, macrophage, and T cell clusters may display increased permissiveness to SARS-CoV-2 invasion. Moreover, DC cell clusters may represent a susceptible target for MERS-CoV, whereas HCoV-229E may target both DC and fibroblast cell clusters.

3.6. Buccal tissue

Buccal tissue was annotated as epithelial, endothelial, fibroblast, smooth muscle cell (SMC), MPS, CD4⁺ T cell (T_{cell}:CD4⁺), CD8⁺ T cell (T_{cell}:CD8⁺), NK cell, B cell, lymphatic cell, mast cell, and Schwann cell (Fig. 6A). Except for BSG, ITGB2, CTSB, and CTSL, the majority of receptors and proteases, such as ACE2, DPP4, ANPEP, CD209, CLEC4G/M, and members of the TMPRSS family (including TMPRSS2, TMPRSS4, and TMPRSS11A), were observed to be expressed at comparatively lower levels within the buccal tissue (Fig. 2C and Additional file 2: Table S2). Our results demonstrated that BSG exhibited a relatively heightened transcriptional levels in most cells (excluding mast cells), whereas ITGB2 manifested a more elevated transcriptional levels in immune cells, particularly in MPS, CD4⁺ T cell, CD8⁺ T cell, and NK cell (Fig. 6B). Analysis of double-positive receptor-protease cells revealed a markedly greater proportion of BSG⁺CTSB⁺ cells in epithelial, fibroblast, and CD4⁺ T cell clusters. Conversely, only fibroblast cell clusters exhibited a significantly higher proportion of BSG⁺CTSL⁺ cells. ITGB2⁺CTSB⁺ cells and ITGB2⁺CTSL⁺ cells were predominantly detected in immune cell clusters, particularly in MPS, CD4⁺ T cell, and CD8⁺ T cell populations (Fig. 6C). However, our study revealed modest levels of RFs observed in the buccal tissue, such as IFITM1-3, LY6E, and CD44 (Fig. 2C and Additional file 2: Table S2), suggesting that buccal tissue exhibited a certain level of defense against HCoV infection. Overall, buccal tissue may serve as a target for SARS-CoV-2 infection, particularly within epithelial, fibroblast, MPS, CD4⁺ T cell, and CD8⁺ T cell clusters. Moreover, the likelihood of buccal infection by other HCoVs (including MERS-CoV, HCoV-229E and HCoV-NL63) appeared to be relatively low.

3.7. Pulp and periodontium

To ensure the reliability of our oral data, we extended our analysis to pulp and periodontal tissues, which were not usually exposed to the external environment. We identified 11 different cell types in the pulp and periodontium: mesenchymal stem cell (MSC) 1, MSC2, MSC3, endothelial, fibroblast, CD4⁺ T cell (T_{cell}:CD4⁺), Schwann cell, MPS, epithelial, NK cell and B cell (Fig. 7A). While ACE2, ASGR1, KREMEN1, ITGB2, DPP4, ANPEP, CD209, CLEC4G/M and TMPRSS2 expression were low in both the tissues and the cell types examined (Fig. 2C and Additional file 2: Table S2). Conversely, BSG with CTSB and CTSL showed higher expression levels in periodontal or pulp tissues (Fig. 2C and 7B and Additional file 2: Table S2). Although the percentage of double-positive receptor-protease cells was slightly higher in the periodontium than in the pulp, this difference was not statistically significant (Fig. 7C). Notably, our analysis showed that RFs such as IFITM1-3, LY6E, CD44, and APOE were widely expressed in both tissues (Fig. 7B), suggesting that they confer resistance to HCoV infection. In conclusions, our results demonstrated that the probability of HCoV infection in pulp and periodontal tissues was low.

Importantly, our study indicated that substitutable receptors, such as BSG, CTSB, and CTSL, may play a critical role in SARS-CoV-2 infection of oral cells, in contrast to confirmed receptors and proteases, such as ACE2 and TMPRSS2. Our findings highlighted the complex tissue-specificity of these genes and suggest that these receptors and proteases may represent an alternative entry pathway for SARS-CoV-2 into oral cells. Moreover, our investigation had unveiled the susceptibility of oral tissues to other HCoVs, namely SARS-CoV, MERS-CoV and HCoV-229E. Generally speaking, oral tissues exhibited a low degree of susceptibility to other HCoVs, which was in line with the rare occurrence of oral symptoms caused by these viruses. Nevertheless, select cell clusters within the oral tissues may be vulnerable to other HCoVs. It is important to note that additional research is required to unravel the fundamental mechanisms underlying such susceptibility.

4. Discussion

Although respiratory failure remained the primary cause of mortality in COVID-19, the deleterious impact of oral symptoms on their overall quality of life should not be underestimated, as they were pervasive and distressing. Therefore, it was imperative to gain a comprehensive understanding of the precise manner in which COVID-19 affected the oral cavity. In a prior research, Huang et al. established SARS-CoV-2 infection in the salivary glands and oral mucosa, thus underscoring the significance of the oral cavity as a site of infection [16]. Based on this premise, we utilized publicly accessible scRNA-seq datasets to scrutinize the basal transcript levels of widespread SCARFs in oral tissues and compiled the first-ever integrated human oral SCARFs scRNA-seq atlas. While it remained challenging to assess the dynamic fluctuations of SCARFs in oral tissues and infer the viral tropism at the RNA levels, our study had furnished insights and orientations for exploring the tropism and pathogenicity of SARS-CoV-2 and other HCoVs in oral tissues.

Consistent with previous studies, our research revealed that ACE2 and TMPRSS2 were primarily expressed in epithelial cells, with only a small fraction of cells expressing ACE2 and/or TMPRSS2. Huang et al. also observed a scarcity of ACE2 and TMPRSS2 co-expression [16]. Conversely, alternative receptors such as BSG and ITGB2, as well as potential proteases such as CTSB and CTSL, exhibited elevated transcript levels. Nonetheless, the expression of SCARFs was subject to diverse influences. Notably, recent research had suggested that ACE2 was an Interferon-stimulated gene (ISG) [66,67]. Chua et al. observed a threefold increase in ACE2 expression levels in epithelial cell clusters following SARS-CoV-2 infection, which was found to be associated with interferon signaling in immune

cells [68]. However, ISGs could directly restrict the virus infection and enhance various innate immune responses [69,70]. Moreover, ACE2 could exert anti-inflammatory and anti-fibrotic effects by inactivating Angiotensin II (Ang II) and prevent ARDS [71,72]. Therefore, SARS-CoV-2 may exploit the host-protective response mediated by ACE2 to facilitate further infection of the host, which could be one of the strategies employed by SARS-CoV-2 to challenge the host [66]. Furthermore, Sajuthi et al. had reported that IL-13-mediated type 2 inflammation in the airway epithelium greatly upregulated the expression of TMPRSS2 [67], implying that the expression of TMPRSS2 may be subject to regulation by the inflammatory responses. In fact, highly pathogenic viruses such as SARS-CoV have been known to target and modulate host innate immune responses, including interfering with interferon signaling, as a means of self-protection [73]. Therefore, further investigation is needed to study the temporal dynamics of SCARFs levels in the host both prior to and following viral infection. Moreover, recent research had suggested that periodontal pathogens/periodontitis may also impact ACE2 expression levels, particularly in relation to *Fusobacterium nucleatum* and *Porphyromonas gingivalis*, which may heighten the potential risk of severe COVID-19 in patients with periodontitis [74–76].

In addition to ACE2 and TMPRSS2, we had observed the widespread expression of BSG, CTSSB, and CTSL in oral tissues/cells, particularly in epithelial cell clusters. In fact, shortly after the discovery of COVID-19, BSG (CD147) has been found to interact with the spike protein of SARS-CoV-2 and mediate SARS-CoV-2 infection [33]. CTSSB/CTSL was first discovered as an entry factor for SARS-CoV infected cells, and subsequently Hoffmann et al. confirmed that CTSSB/CTSL can also serve as an entry factor for SARS-CoV-2 [18]. Here, we conducted a quantitative analysis of the expression of BSG, CTSSB, and CTSL in the oral cavity and found that their expression was relatively high compared to other alternative entry factors, which may be the main alternative entry factors. Currently, some studies have found inhibitors that may be effective against these alternative entry factors. Anti-CD147 antibody, Meplazumab, could effectively inhibit viral entry and inflammation caused by SARS-CoV-2 and its variants [33,77]. Additionally, studies suggested beneficial effects of azithromycin in reducing viral load of hospitalized patients, possibly interfering with ligand/CD147 receptor interactions [78]. Chloroquine or hydroxy-chloroquine are already used against COVID-19, inhibiting the activity of CTSSB/CTSL non-specifically [79]. K777 and E64d were found to effectively inhibit CTSSB/CTSL, blocking CTSSB/CTSL mediated entry pathways and exerting anti SARS-CoV-2 effect [18,80]. Therefore, these inhibitors for alternative entry factors BSG and CTSSB/CTSL are likely to be employed to treat oral COVID-19 symptoms. In contrast, our results demonstrated that ITGB2 [also known as Lymphocyte Function-associated Antigen 1 (LFA-1)], a leukocyte cell adhesion molecule, was primarily expressed in immune cell clusters, particularly MPS and CD4⁺ T cells. Previously, Shen et al. had already found that SARS-CoV-2 may infect host CD4⁺ T cells via ITGB2 instead of ACE2 and TMPRSS2, resulting in CD4⁺ T cell dysfunction and depletion. Infected T cells may lose their cytotoxicity against the virus and may also disseminate the virus to different systemic locations through the circulation, thereby aggravating the disease [50]. These findings implied that immune cells in the oral cavity, particularly MPS and CD4⁺ T cells, were susceptible to SARS-CoV-2 infection. Thus, it is of paramount importance for COVID-19 patients to take proper oral management in their daily lives, such as gargling and tooth cleaning [81,82]. Additionally, replication factor ZCRB1 and assembly and trafficking factors were widely expressed in oral cells, suggesting that most cells in the oral cavity were capable of facilitating HCoV replication, assembly and trafficking.

Furthermore, we conducted double positive cell analyses on the co-expression of receptors and enzymes. We found that oral epithelial cells seem to be more inclined to co express receptors and enzymes compared to other cells, indicating that epithelial cells as a protective barrier for oral cavity may be more susceptible to HCoVs, which is consistent with the higher incidence of mucosal lesions in COVID-19 patients [10,13]. In addition, we also found that there may be synergistic enrichment between receptors and enzymes. For example, in tongue, BSG⁺CTSSB⁺ cells and BSG⁺CTSL⁺ cells are predominantly present in epithelial cells, fibroblast cells, endothelial cells and MPS, while BSG, CTSSB, and CTSL are mainly expressed in these cells as well (Fig. 4D and E). Similar situations exist not only in the oral cavity, but also in other regions of the oral cavity, indicating a synergistic enrichment of BSG, CTSSB, and CTSL. Similarly, ITGB2⁺CTSSB⁺ cells and ITGB2⁺CTSL⁺ cells are predominantly present in MPS, suggesting that ITGB2, CTSSB and CTSL may be synergistically enriched in MPS. Thus, these findings suggest that all cell types in the oral cavity, including epithelial, immune, and connective tissue cell clusters, are susceptible to SARS-CoV-2 infection, with epithelial cells being the most vulnerable as the primary protective barrier.

In addition to factors that facilitate viral infection and replication, we also investigated the basal expression levels of restriction factors in the oral cavity. Host restriction factors are specialized, widely expressed antiviral factors that can block the replication of viruses during their life cycle in host cells [17,20,37]. Buchrieser et al. confirmed that IFITM1-3 can serve as antiviral factors for SARS-CoV-2, blocking the entry of SARS-CoV-2 and inhibiting S-mediated fusion, with IFITM1 being more active than IFITM2 and IFITM3 [58]. Pfaender et al. demonstrated that LY6E was a critical antiviral immune effector that controlled HCoVs (including SARS-CoV, SARS-CoV-2 and MERS-CoV) infection and pathogenesis by interfering with spike protein-mediated membrane fusion [54]. Our findings revealed that restriction factors were widely expressed in oral cells, particularly IFITM1-3 and LY6E, which indicated that IFITM1-3 and LY6E may serve as the key antiviral factors in the oral cavity, aiding the host's resistance against HCoVs infection. Further, these restriction factors, such as IFITMs and LY6E, were typically components of the host's innate immune responses and can be induced by interferon signaling [83,84]. Nevertheless, studies had suggested that IFITM3 may enhance the infectivity of HCoV-OC43 [85], and structural modifications in IFITM3 may intensify the infectivity of SARS-CoV and/or MERS-CoV [86]. LY6E had been shown to enhance the entry of various enveloped viruses into host cells, including influenza A virus, yellow fever virus and human immunodeficiency virus (HIV) [83,87]. Moreover, Shi et al. found that TMPRSS2 overexpression may counteract the IFITM3-mediated restriction of SARS-CoV-2 [88]. Remarkably, HCoVs had evolved mechanisms to counteract host restriction factors, such as using viral proteins to antagonize host restriction functions, indicating a coevolutionary arms race between viruses and hosts [17,84,89,90]. While our research only examined the basal transcript levels of restriction factors, this could be a critical determinant of oral tissues susceptibility to viral infection.

Our investigation had revealed that MSG exhibited high levels of expression for BSG, CTSB, and CTSL, while displaying low levels for IFITMs and LY6E (Fig. 2C). These findings suggested that MSG could be vulnerable to SARS-CoV-2 infection. Furthermore, our results had demonstrated that acinar and ductal epithelial cells of MSG displayed high susceptibility to SARS-CoV-2 (Fig. 3B–D). Since epithelial cells are responsible for saliva secretion and excretion functions, this observation might clarify the pathogenesis of xerostomia as the most prevalent COVID-19 oral symptom, which corresponded to the outcomes observed in clinical practice [10,13]. It is noteworthy that, despite being a salivary gland, PG expressed low levels of receptors and proteases, which was consistent with the low incidence of sialadenitis observed in COVID-19 patients [10] (Fig. 2C). Furthermore, high transcript levels of BSG, CTSB, and CTSL were observed in the tongue, specifically in epithelial cells. Remarkably, the expression levels of the restriction factors IFITM2-3 and LY6E were also high in the tongue, which could potentially act as a protective mechanism for tongue against HCoVs infection. The etiology of dysgeusia in COVID-19 patients was primarily attributed to the infection of taste bud cells by SARS-CoV-2 [91]. As such, our research could shed light on the reason why some COVID-19 patients did not manifest with taste disorders. However, SCARFs expression patterns were more intricate in other parts of the oral cavity, such as gingiva, buccal, pulp, and periodontium. Subsequent studies could be conducted at the cellular level to verify the expression levels of some important alternative entry factors such as BSG, ITGB2, CTSB and CTSL. Further, overexpressing or reducing the expression level of alternative entry factors in cells and detecting whether the entry of HCoVs into the cells was affected and whether it was consistent with our bioinformatics analysis. Thus, further investigations or experiments are warranted to validate the expression patterns of SCARFs in the oral cavity and elucidate their potential impact on viral pathogenesis within the oral cavity.

Although our study focused primarily on SARS-CoV-2, it provided direction for investigating the oral tropism of other HCoVs,

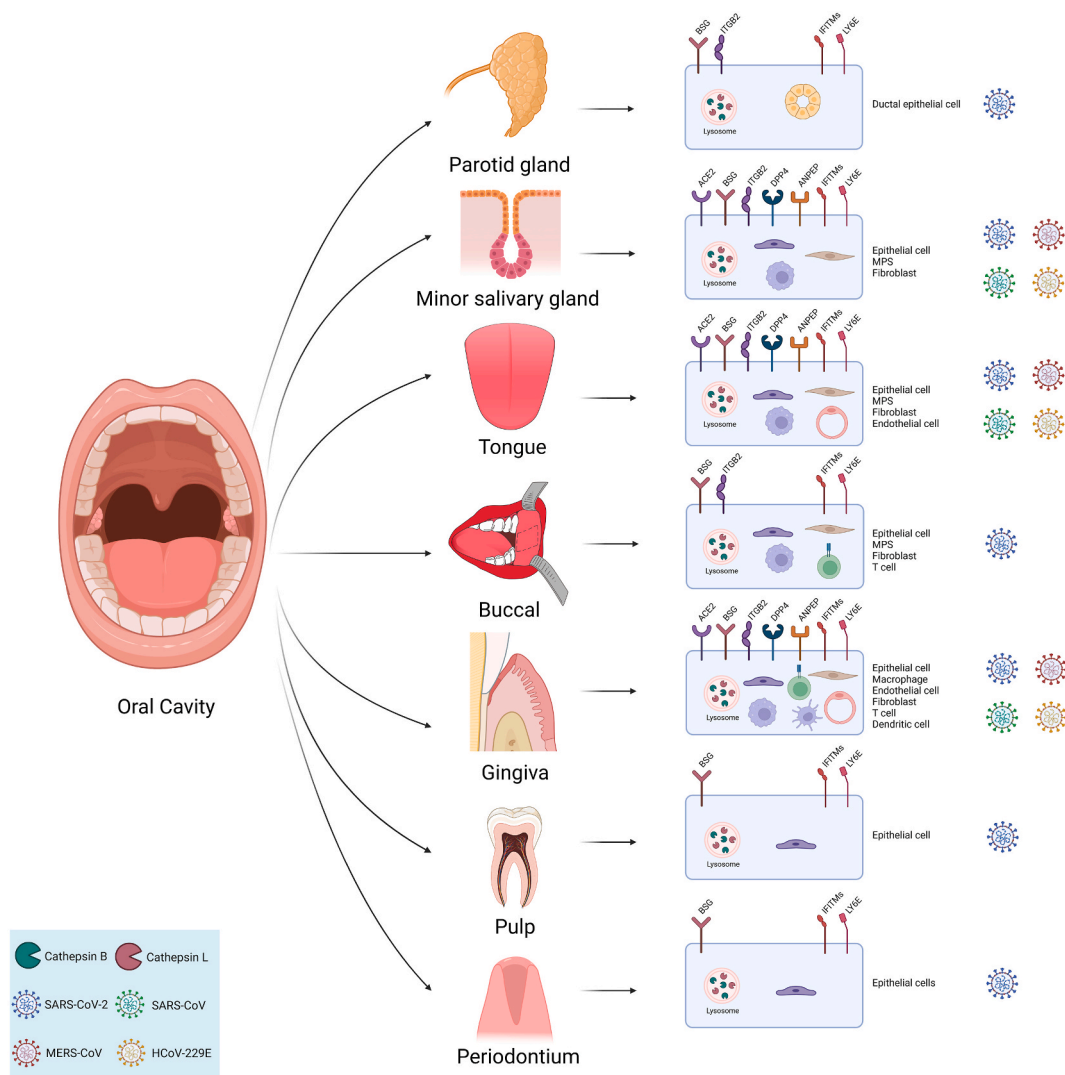


Fig. 8. The differential expression profiles of SCARFs across diverse regions of the oral cavity and the cell types that demonstrated heightened susceptibility to HCoVs infection (figure was created with [Biorender.com](https://www.biorender.com)).

including SARS-CoV, MERS-CoV, HCoV-NL63, and HCoV-229E. Compared to BSG, the expression levels of the receptors/alternative receptors for these coronaviruses, such as ACE2 (SARS-CoV and HCoV-NL63), DPP4 (MERS-CoV), ANPEP (HCoV-229E), CD209 (SARS-CoV), and CLEC4M/G (SARS-CoV), were relatively low in oral tissues, suggesting that oral tissues may be less susceptible to MERS-CoV, HCoV-229E, and SARS-CoV. However, certain cell types within oral tissues may exhibit heightened susceptibility to infection by HCoVs. All in all, serous epithelial cell and ductal epithelial cell in MSG exhibited a greater degree of susceptibility to MERS-CoV, whereas ductal epithelial cell in MSG and MPS in tongue were the most susceptible to HCoV-229E. As our investigation did not encompass the proteases utilized by HCoV-NL63 for host cell entry, nor the receptors utilized by HCoV-OC43 and HCoV-HKU1 for cell entry [17], our findings may be deemed unreliable for predicting the tropism of these three coronaviruses for oral tissues (Fig. 8 and Table 1).

Our study revealed the expression patterns of SCARFs in oral cavity based on scRNA-seq analysis, which can help us understand and explore underlying mechanisms of HCoVs infection in the oral cavity. However, there are some limitations of this study. Firstly, our research is only a bioinformatics analysis, which requires further experimental verification. Secondly, our study lacks dynamic infection models of the virus to observe how the expression levels of SCARFs change as the HCoVs infection progresses. However, this modeling of HCoVs infection requires relatively high experimental conditions and P3 laboratory. Thirdly, we lack the collection of oral tissues from infected patients to further validate the expression levels of SCARFs and to establish patient datasets, and subsequent studies could consider scraping epithelial cells from some regions of the infected patients' oral cavity for comparative analysis.

In summary, based on the results of our study, we found that BSG, CTSB, and CTSL may give the biggest contribution to the oral tropism of SARS-CoV-2. This is because they are widely distributed and have the highest expression level in oral tissue, and the proportion of BSG⁺CTSB⁺ cells or BSG⁺CTSL⁺ cells is the highest among double positive cells.

5. Conclusions

The aim of this study was to gain insight into the expression levels of SCARFs in seven types of oral tissues (including MSG, PG, tongue, gingiva, buccal tissue, periodontium, and pulp) and potential HCoVs targets in oral tissues and cells. Based on our analysis, BSG, CTSB, and CTSL exhibited enrichment in oral tissues. Conversely, it appeared that various SCARFs, including ACE2, ASGR1, KREMEN1, DPP4, ANPEP, CD209, CLEC4G/M, TMPRSS family proteins (including TMPRSS2, TMPRSS4, and TMPRSS11A), and FURIN, were expressed at low levels in the oral cavity. Our study also demonstrated widespread expression of restriction factors, particularly IFITM1-3 and LY6E, in oral cells. Additionally, some replication, assembly, and trafficking factors appeared to exhibit broad oral tissues expression patterns. Overall, the extensive expression of SCARFs across MSG cell clusters suggested a high susceptibility to SARS-CoV-2 infection in MSG, while tongue expressed a combination of factors that both facilitate and impede SARS-CoV-2 infection. Additionally, MSG presented a putative target for the pathogenic assault of MERS-CoV, SARS-CoV, and HCoV-229E, while tongue may similarly exhibit heightened susceptibility to HCoV-229E infection. In contrast, PG, gingiva, buccal tissue, periodontium, and pulp generally showed a trend of low expression levels of entry factors and high expression levels of restriction factors, indicating that these tissues may not be susceptible to HCoVs infection. Our findings had yielded preliminary insights into the underlying mechanisms that contributed to the potential risk of HCoVs infection in the oral cavity and the elevated incidence of oral symptoms associated with COVID-19, offering evidence for dental clinical practice, treatment, and prevention strategies in daily life. Hence, our study served as a valuable and utilitarian resource for future clinical research on the basic biology of SARS-CoV-2 and other coronaviruses as well as the pathology and treatment of COVID-19.

Ethics approval and consent to participate

Not applicable.

Consent for publication

All the authors read and approved the final version of the manuscript.

Funding

This study was financially supported by the Fundamental Research Fund of Science and Technology Foundation of Shenzhen City

Table 1

Human coronavirus tropism for oral cavity.

	SARS-CoV-2	SARS-CoV	MERS-CoV	HCoV-229E
MSG	Epithelial cell, MPS	Epithelial cell	Epithelial cell	Epithelial cell, fibroblast
PG	Ductal epithelial cell	NA	NA	NA
Tongue	Epithelial cell, fibroblast, endothelial cell, MPS	Epithelial cell	Fibroblast	MPS
Gingiva	Epithelial cell, endothelial cell, macrophage, T cell	Epithelial cell	Dendritic cell	Dendritic cell, fibroblast
Buccal	Epithelial cell, fibroblast, MPS, CD4 ⁺ T cell, CD8 ⁺ T cell	NA	NA	NA
Pulp and periodontium	Epithelial cell	NA	NA	NA

(Key program JCYJ20220818095811026) and Shenzhen Science and Technology Innovation Commission stable support project (Grant No. 20220810174028001).

Data availability statement

The available data generated or analyzed during this study are included in this published article and its supplementary information files. Individual data are available from the corresponding author on reasonable request. This study also used publicly available datasets from GEO (GSE172577, GSE161267 and GSE188478) and COVID-19 Cell Atlas website (<https://www.covid19cellatlas.org/>).

CRedit authorship contribution statement

Feng Gao: Writing – review & editing, Writing – original draft, Visualization, Validation, Supervision, Project administration, Formal analysis, Data curation. **Weiming Lin:** Writing – review & editing, Writing – original draft, Visualization, Validation, Methodology, Formal analysis, Data curation. **Xia Wang:** Writing – review & editing, Writing – original draft, Visualization, Validation, Supervision, Conceptualization. **Mingfeng Liao:** Validation, Methodology, Formal analysis. **Mingxia Zhang:** Validation, Methodology, Formal analysis, Data curation. **Nianhong Qin:** Software, Methodology, Formal analysis, Data curation. **Xianxiang Chen:** Methodology, Formal analysis. **Lixin Xia:** Software, Methodology, Formal analysis. **Qianming Chen:** Writing – review & editing, Visualization, Validation, Supervision, Data curation, Conceptualization. **Ou Sha:** Writing – review & editing, Writing – original draft, Visualization, Validation, Supervision, Funding acquisition, Formal analysis, Data curation, Conceptualization.

Declaration of competing interest

The authors declare that they have no known competing financial interests or personal relationships that could have appeared to influence the work reported in this paper.

Appendix A. Supplementary data

Supplementary data to this article can be found online at <https://doi.org/10.1016/j.heliyon.2024.e28280>.

Abbreviations

SCARFs	SARS-CoV-2 and coronavirus-associated receptors and factors
SARS-CoV-2	Severe Acute Respiratory Syndrome Coronavirus-2
SARS-CoV	Severe Acute Respiratory Syndrome Coronavirus
MERS-CoV	Middle East Respiratory Syndrome Coronavirus
HCoVs	Human coronavirus
COVID-19	Coronavirus Disease 2019
scrRNA-seq	Single-cell RNA sequencing
UMAP	Uniform manifold approximation and projection
GEO	Gene Expression Omnibus
ACE2	Angiotensin-converting enzyme 2
TMPRSS2	Transmembrane serine protease 2
BSG	Basignin
CTSB	Cathepsin B
CTSL	Cathepsin L
RF	Restriction factor
MSG	Minor salivary gland
PG	Parotid gland
MPS	Mononuclear phagocyte system
DC	Dendritic cell
SMC	Smooth muscle cell
MSC	Mesenchymal stem cell
ARDS	Acute respiratory distress syndrome
MODS	Multiple organ dysfunction syndrome
LFA-1	Lymphocyte function-associated antigen 1
ISG	Interferon-stimulated gene
Ang II	Angiotensin II

References

- [1] C. Huang, Y. Wang, X. Li, L. Ren, J. Zhao, Y. Hu, et al., Clinical features of patients infected with 2019 novel coronavirus in Wuhan, China, *Lancet* 395 (2020) 497–506, [https://doi.org/10.1016/S0140-6736\(20\)30183-5](https://doi.org/10.1016/S0140-6736(20)30183-5).
- [2] P. Zhou, X.-L. Yang, X.-G. Wang, B. Hu, L. Zhang, W. Zhang, et al., A pneumonia outbreak associated with a new coronavirus of probable bat origin, *Nature* 579 (2020) 270–273, <https://doi.org/10.1038/s41586-020-2012-7>.
- [3] S.W.X. Ong, Y.K. Tan, P.Y. Chia, T.H. Lee, O.T. Ng, M.S.Y. Wong, et al., Air, surface Environmental, and personal protective Equipment contamination by severe acute respiratory syndrome coronavirus 2 (SARS-CoV-2) from a Symptomatic patient, *JAMA* 323 (2020) 1610–1612, <https://doi.org/10.1001/jama.2020.3227>.
- [4] A.G. Harrison, T. Lin, P. Wang, Mechanisms of SARS-CoV-2 transmission and pathogenesis, *Trends Immunol.* 41 (2020) 1100–1115, <https://doi.org/10.1016/j.it.2020.10.004>.
- [5] Z.-W. Ye, S. Yuan, K.-S. Yuen, S.-Y. Fung, C.-P. Chan, D.-Y. Jin, Zoonotic origins of human coronaviruses, *Int. J. Biol. Sci.* 16 (2020) 1686–1697, <https://doi.org/10.7150/ijbs.45472>.
- [6] N. Chen, M. Zhou, X. Dong, J. Qu, F. Gong, Y. Han, et al., Epidemiological and clinical characteristics of 99 cases of 2019 novel coronavirus pneumonia in Wuhan, China: a descriptive study, *Lancet* 395 (2020) 507–513, [https://doi.org/10.1016/S0140-6736\(20\)30211-7](https://doi.org/10.1016/S0140-6736(20)30211-7).
- [7] E. de Wit, N. van Doremalen, D. Falzarano, V.J. Munster, SARS and MERS: recent insights into emerging coronaviruses, *Nat. Rev. Microbiol.* 14 (2016) 523–534, <https://doi.org/10.1038/nrmicro.2016.81>.
- [8] A. Zumla, D.S. Hui, S. Perlman, Middle East respiratory syndrome, *Lancet* 386 (2015) 995–1007, [https://doi.org/10.1016/S0140-6736\(15\)60454-8](https://doi.org/10.1016/S0140-6736(15)60454-8).
- [9] A. Assiri, J.A. Al-Tawfiq, A.A. Al-Rabeeah, F.A. Al-Rabiah, S. Al-Hajjar, A. Al-Barrak, et al., Epidemiological, demographic, and clinical characteristics of 47 cases of Middle East respiratory syndrome coronavirus disease from Saudi Arabia: a descriptive study, *Lancet Infect. Dis.* 13 (2013) 752–761, [https://doi.org/10.1016/S1473-3099\(13\)70204-4](https://doi.org/10.1016/S1473-3099(13)70204-4).
- [10] J. Amorim dos Santos, A.G.C. Normando, R.L. Carvalho da Silva, A.C. Acevedo, G. De Luca Canto, N. Sugaya, et al., Oral manifestations in patients with COVID-19: a 6-month update, *J. Dent. Res.* 100 (2021) 1321–1329, <https://doi.org/10.1177/00220345211029637>.
- [11] W. Lin, F. Gao, X. Wang, N. Qin, X. Chen, K.Y. Tam, et al., The oral manifestations and related mechanisms of COVID-19 caused by SARS-CoV-2 infection, *Front. Cell. Neurosci.* 16 (2023), <https://doi.org/10.3389/fncel.2022.1006977>.
- [12] D.M. El Kady, E.A. Gomaa, W.S. Abdella, R. Ashraf Hussien, R.H. Abd ElAziz, A.G.A. Khater, Oral manifestations of COVID-19 patients: an online survey of the Egyptian population, *Clinical and Experimental Dental Research* 7 (2021) 852–860, <https://doi.org/10.1002/cre2.429>.
- [13] H. Farid, M. Khan, S. Jamal, R. Ghafoor, Oral manifestations of Covid-19-A literature review, *Rev. Med. Virol.* 32 (2022) e2248, <https://doi.org/10.1002/rmv.2248>.
- [14] P. Sharma, S. Malik, V. Wadhwan, S. Gotur Palakshappa, R. Singh, Prevalence of oral manifestations in COVID-19: a systematic review, *Rev. Med. Virol.* 32 (2022) e2345, <https://doi.org/10.1002/rmv.2345>.
- [15] S.R. Stein, S.C. Ramelli, A. Grazioli, J.Y. Chung, M. Singh, C.K. Yinda, et al., SARS-CoV-2 infection and persistence in the human body and brain at autopsy, *Nature* 612 (2022) 758–763, <https://doi.org/10.1038/s41586-022-05542-y>.
- [16] N. Huang, P. Pérez, T. Kato, Y. Mikami, K. Okuda, R.C. Gilmore, et al., SARS-CoV-2 infection of the oral cavity and saliva, *Nat. Med.* 27 (2021) 892–903, <https://doi.org/10.1038/s41591-021-01296-8>.
- [17] J.P. Evans, S.-L. Liu, Role of host factors in SARS-CoV-2 entry, *J. Biol. Chem.* 297 (2021) 100847, <https://doi.org/10.1016/j.jbc.2021.100847>.
- [18] M. Hoffmann, H. Kleine-Weber, S. Schroeder, N. Krüger, T. Herrler, S. Erichsen, et al., SARS-CoV-2 cell entry depends on ACE2 and TMPRSS2 and is blocked by a clinically proven protease inhibitor, *Cell* 181 (2020) 271–280, <https://doi.org/10.1016/j.cell.2020.02.052>.
- [19] J.-E. Park, K. Li, A. Barlan, A.R. Fehr, S. Perlman, P.B. McCray, et al., Proteolytic processing of Middle East respiratory syndrome coronavirus spikes expands virus tropism, *Proc. Natl. Acad. Sci. USA* 113 (2016) 12262–12267, <https://doi.org/10.1073/pnas.1608147113>.
- [20] C.B. Jackson, M. Farzan, B. Chen, H. Choe, Mechanisms of SARS-CoV-2 entry into cells, *Nat. Rev. Mol. Cell Biol.* 23 (2022) 3–20, <https://doi.org/10.1038/s41580-021-00418-x>.
- [21] V.S. Raj, H. Mou, S.L. Smits, D.H.W. Dekkers, M.A. Müller, R. Dijkman, et al., Dipeptidyl peptidase 4 is a functional receptor for the emerging human coronavirus EMC, *Nature* 495 (2013) 251–254, <https://doi.org/10.1038/nature12005>.
- [22] T. Ou, H. Mou, L. Zhang, A. Ojha, H. Choe, M. Farzan, Hydroxychloroquine-mediated inhibition of SARS-CoV-2 entry is attenuated by TMPRSS2, *PLoS Pathog.* 17 (2021) e1009212, <https://doi.org/10.1371/journal.ppat.1009212>.
- [23] K. Bollavaram, T.H. Leeman, M.W. Lee, A. Kulkarni, S.G. Upshaw, J. Yang, et al., Multiple sites on SARS-CoV-2 spike protein are susceptible to proteolysis by cathepsins B, K, L, S, and V, *Protein Sci.* 30 (2021) 1131–1143, <https://doi.org/10.1002/pro.4073>.
- [24] M.-M. Zhao, W.-L. Yang, F.-Y. Yang, L. Zhang, W.-J. Huang, W. Hou, et al., Cathepsin L plays a key role in SARS-CoV-2 infection in humans and humanized mice and is a promising target for new drug development, *Signal Transduct. Targeted Ther.* 6 (2021) 134, <https://doi.org/10.1038/s41392-021-00558-8>.
- [25] M. Hoffmann, H. Kleine-Weber, S. Pöhlmann, A multibasic cleavage site in the spike protein of SARS-CoV-2 is essential for infection of human lung cells, *Mol. Cell* 78 (2020) 779–784, <https://doi.org/10.1016/j.molcel.2020.04.022>. e775.
- [26] K. Shirato, M. Kawase, S. Matsuyama, Wild-type human coronaviruses prefer cell-surface TMPRSS2 to endosomal cathepsins for cell entry, *Virology* 517 (2018) 9–15, <https://doi.org/10.1016/j.virol.2017.11.012>.
- [27] K. Shirato, K. Kanou, M. Kawase, S. Matsuyama, Clinical isolates of human coronavirus 229E bypass the endosome for cell entry, *J. Virol.* 91 (2017) e01387-01316, <https://doi.org/10.1128/JVI.01387-16>.
- [28] S. Bertram, R. Dijkman, M. Habjan, A. Heurich, S. Gierer, I. Glowacka, et al., TMPRSS2 activates the human coronavirus 229E for cathepsin-independent host cell entry and is expressed in viral target cells in the respiratory epithelium, *J. Virol.* 87 (2013) 6150–6160, <https://doi.org/10.1128/JVI.03372-12>.
- [29] A. Milewska, P. Nowak, K. Owczarek, A. Szczepanski, M. Zarebski, A. Hoang, et al., Entry of human coronavirus NL63 into the cell, *J. Virol.* 92 (2018) e01933-01917, <https://doi.org/10.1128/JVI.01933-17>.
- [30] J.K. Millet, G.R. Whittaker, Host cell entry of Middle East respiratory syndrome coronavirus after two-step, furin-mediated activation of the spike protein, *Proc. Natl. Acad. Sci. USA* 111 (2014) 15214–15219, <https://doi.org/10.1073/pnas.1407087111>.
- [31] M. Zhong, B. Lin, J.L. Pathak, H. Gao, A.J. Young, X. Wang, et al., ACE2 and furin expressions in oral epithelial cells possibly facilitate COVID-19 infection via respiratory and fecal–oral routes, *Front. Med.* 7 (2020), <https://doi.org/10.3389/fmed.2020.580796>.
- [32] Y. Sawa, S. Ibaragi, T. Okui, J. Yamashita, T. Ikebe, H. Harada, Expression of SARS-CoV-2 entry factors in human oral tissue, *J. Anat.* 238 (2021) 1341–1354, <https://doi.org/10.1111/joa.13391>.
- [33] K. Wang, W. Chen, Z. Zhang, Y. Deng, J.-Q. Lian, P. Du, et al., CD147-spike protein is a novel route for SARS-CoV-2 infection to host cells, *Signal Transduct. Targeted Ther.* 5 (2020) 283, <https://doi.org/10.1038/s41392-020-00426-x>.
- [34] R. Zang, M.F. Gomez Castro, B.T. McCune, Q. Zeng, P.W. Rothlauf, N.M. Sonnek, et al., TMPRSS2 and TMPRSS4 promote SARS-CoV-2 infection of human small intestinal enterocytes, *Sci Immunol* 5 (2020), <https://doi.org/10.1126/sciimmunol.abc3582>.
- [35] P. Zmora, M. Hoffmann, H. Kollmus, A.-S. Moldenhauer, O. Danov, A. Braun, et al., TMPRSS11A activates the influenza A virus hemagglutinin and the MERS coronavirus spike protein and is insensitive against blockade by HAI-1, *J. Biol. Chem.* 293 (2018) 13863–13873, <https://doi.org/10.1074/jbc.RA118.001273>.
- [36] G. Jocher, V. Grass, S.K. Tschirner, L. Riepler, S. Breimann, T. Kaya, et al., ADAM10 and ADAM17 promote SARS-CoV-2 cell entry and spike protein-mediated lung cell fusion, *EMBO Rep.* 23 (2022) e54305, <https://doi.org/10.15252/embr.202154305>.
- [37] S.F. Kluge, D. Sauter, F. Kirchhoff, Snapshot: antiviral restriction factors, *Cell* 163 (2015) 774, <https://doi.org/10.1016/j.cell.2015.10.019>, 774.e771.
- [38] K.R. Prasanth, M. Hirano, W.S. Fagg, E.T. McAnarney, C. Shan, X. Xie, et al., Topoisomerase III- β is required for efficient replication of positive-sense RNA viruses, *Antivir. Res.* 182 (2020) 104874, <https://doi.org/10.1016/j.antiviral.2020.104874>.
- [39] M. Singh, V. Bansal, C. Feschotte, A single-cell RNA expression map of human coronavirus entry factors, *Cell Rep.* 32 (2020) 108175, <https://doi.org/10.1016/j.celrep.2020.108175>.

- [40] H. Xu, L. Zhong, J. Deng, J. Peng, H. Dan, X. Zeng, et al., High expression of ACE2 receptor of 2019-nCoV on the epithelial cells of oral mucosa, *Int. J. Oral Sci.* 12 (2020) 8, <https://doi.org/10.1038/s41368-020-0074-x>.
- [41] T. Stuart, A. Butler, P. Hoffman, C. Hafemeister, E. Papalexi, W.M. Mauck III, et al., Comprehensive integration of single-cell data, *Cell* 177 (2019) 1888–1902, <https://doi.org/10.1016/j.cell.2019.05.031>. e1821.
- [42] P. Germain, A. Lun, C. Garcia Meixide, W. Macnair, M. Robinson, Doublet identification in single-cell sequencing data using scDblFinder [version 2; peer review: 2 approved, F1000Research 10 (2022), <https://doi.org/10.12688/f1000research.73600.2>.
- [43] I. Korsunsky, N. Millard, J. Fan, K. Slowikowski, F. Zhang, K. Wei, et al., Fast, sensitive and accurate integration of single-cell data with Harmony, *Nat. Methods* 16 (2019) 1289–1296, <https://doi.org/10.1038/s41592-019-0619-0>.
- [44] D. Aran, A.P. Looney, L. Liu, E. Wu, V. Fong, A. Hsu, et al., Reference-based analysis of lung single-cell sequencing reveals a transitional profibrotic macrophage, *Nat. Immunol.* 20 (2019) 163–172, <https://doi.org/10.1038/s41590-018-0276-y>.
- [45] M. Andreatta, S.J. Carmona, UCell: robust and scalable single-cell gene signature scoring, *Comput. Struct. Biotechnol. J.* 19 (2021) 3796–3798, <https://doi.org/10.1016/j.csbj.2021.06.043>.
- [46] W. Guo, D. Wang, S. Wang, Y. Shan, C. Liu, J. Gu, scCancer: a package for automated processing of single-cell RNA-seq data in cancer, *Briefings Bioinform.* 22 (2020), <https://doi.org/10.1093/bib/bbaa127>.
- [47] COVID-19 cell atlas. <https://www.covid19cellatlas.org/index.healthy.html>, 20 May 2022.
- [48] GitHub. <https://github.com/bansalvi/COVID19-SCARFs>, 20 May 2022.
- [49] Y. Gu, J. Cao, X. Zhang, H. Gao, Y. Wang, J. Wang, et al., Receptome profiling identifies KREMEN1 and ASGR1 as alternative functional receptors of SARS-CoV-2, *Cell Res.* 32 (2022) 24–37, <https://doi.org/10.1038/s41422-021-00595-6>.
- [50] X.R. Shen, R. Geng, Q. Li, Y. Chen, S.F. Li, Q. Wang, et al., ACE2-independent infection of T lymphocytes by SARS-CoV-2, *Signal Transduct. Targeted Ther.* 7 (2022) 83, <https://doi.org/10.1038/s41392-022-00919-x>.
- [51] R. Amraei, W. Yin, M.A. Napoleon, E.L. Suder, J. Berrigan, Q. Zhao, et al., CD209L/L-SIGN and CD209/DC-SIGN act as receptors for SARS-CoV-2, *ACS Cent. Sci.* 7 (2021) 1156–1165, <https://doi.org/10.1021/acscentsci.0c01537>.
- [52] D. Hoffmann, S. Mreiter, Y. Jin Oh, V. Montell, E. Elder, R. Zhu, et al., Identification of lectin receptors for conserved SARS-CoV-2 glycosylation sites, *EMBO J.* 40 (2021) e108375, <https://doi.org/10.15252/embj.2021108375>.
- [53] G. Tang, Z. Liu, D. Chen, Human coronaviruses: origin, host and receptor, *J. Clin. Virol.* 155 (2022) 105246, <https://doi.org/10.1016/j.jcv.2022.105246>.
- [54] S. Pfander, K.B. Mar, E. Michailidis, A. Kratzel, I.N. Boys, P. V'kovski, et al., LY6E impairs coronavirus fusion and confers immune control of viral disease, *Nature Microbiology* 5 (2020) 1330–1339, <https://doi.org/10.1038/s41564-020-0769-y>.
- [55] S.B. Biering, S.A. Sarnik, E. Wang, J.R. Zengel, S.R. Leist, A. Schäfer, et al., Genome-wide bidirectional CRISPR screens identify mucins as host factors modulating SARS-CoV-2 infection, *Nat. Genet.* 54 (2022) 1078–1089, <https://doi.org/10.1038/s41588-022-01131-x>.
- [56] H. Zhang, L. Shao, Z. Lin, Q.-X. Long, H. Yuan, L. Cai, et al., APOE interacts with ACE2 inhibiting SARS-CoV-2 cellular entry and inflammation in COVID-19 patients, *Signal Transduct. Targeted Ther.* 7 (2022) 261, <https://doi.org/10.1038/s41392-022-01118-4>.
- [57] A. Mac Kain, G. Maarif, S.-M. Aicher, N. Arhel, A. Baidaliuk, S. Munier, et al., Identification of DAXX as a restriction factor of SARS-CoV-2 through a CRISPR/Cas9 screen, *Nat. Commun.* 13 (2022) 2442, <https://doi.org/10.1038/s41467-022-30134-9>.
- [58] J. Buchrieser, J. Duflo, M. Hubert, B. Monel, D. Planas, M.M. Rajah, et al., Syncytia formation by SARS-CoV-2-infected cells, *EMBO J.* 39 (2020) e106267, <https://doi.org/10.15252/embj.2020106267>.
- [59] D.E. Gordon, G.M. Jang, M. Bouhaddou, J. Xu, K. Obernier, K.M. White, et al., A SARS-CoV-2 protein interaction map reveals targets for drug repurposing, *Nature* 583 (2020) 459–468, <https://doi.org/10.1038/s41586-020-2286-9>.
- [60] L. Cantuti-Castelvetri, R. Ojha, L.D. Pedro, M. Djannatjan, J. Franz, S. Kuivanen, et al., Neuropilin-1 facilitates SARS-CoV-2 cell entry and infectivity, *Science* 370 (2020) 856–860, <https://doi.org/10.1126/science.abd2985>.
- [61] A.C. Walls, Y.-J. Park, M.A. Tortorici, A. Wall, A.T. McGuire, D. Velesler, Structure, function, and antigenicity of the SARS-CoV-2 spike glycoprotein, *Cell* 181 (2020) 281–292, e286, <https://doi.org/10.1016/j.cell.2020.02.058>.
- [62] L. Nguyen, K.A. McCord, D.T. Bui, K.M. Bouwman, E.N. Kitova, M. Elaiha, et al., Sialic acid-containing glycolipids mediate binding and viral entry of SARS-CoV-2, *Nat. Chem. Biol.* 18 (2022) 81–90, <https://doi.org/10.1038/s41589-021-00924-1>.
- [63] D.T. Montoro, A.L. Haber, M. Biton, V. Vinarsky, B. Lin, S.E. Birket, et al., A revised airway epithelial hierarchy includes CFTR-expressing ionocytes, *Nature* 560 (2018) 319–324, <https://doi.org/10.1038/s41586-018-0393-7>.
- [64] L.W. Plasschaert, R. Zilionis, R. Choo-Wing, V. Savova, J. Kneht, G. Roma, et al., A single-cell atlas of the airway epithelium reveals the CFTR-rich pulmonary ionocyte, *Nature* 560 (2018) 377–381, <https://doi.org/10.1038/s41586-018-0394-6>.
- [65] B.F. Matuck, M. Dolnikoff, A.N. Duarte-Neto, G. Maia, S.C. Gomes, D.I. Sendyk, et al., Salivary glands are a target for SARS-CoV-2: a source for saliva contamination, *J. Pathol.* 254 (2021) 239–243, <https://doi.org/10.1002/path.5679>.
- [66] C.G.K. Ziegler, S.J. Allon, S.K. Nyquist, I.M. Mbanjo, V.N. Miao, C.N. Tzouanas, et al., SARS-CoV-2 receptor ACE2 is an interferon-stimulated gene in human airway epithelial cells and is detected in specific cell subsets across tissues, *Cell* 181 (2020) 1016–1035, e1019, <https://doi.org/10.1016/j.cell.2020.04.035>.
- [67] S.P. Sajuthi, P. DeFord, Y. Li, N.D. Jackson, M.T. Montgomery, J.L. Everman, et al., Type 2 and interferon inflammation regulate SARS-CoV-2 entry factor expression in the airway epithelium, *Nat. Commun.* 11 (2020) 5139, <https://doi.org/10.1038/s41467-020-18781-2>.
- [68] R.L. Chua, S. Lukassen, S. Trump, B.P. Hennig, D. Wendisch, F. Pott, et al., COVID-19 severity correlates with airway epithelium-immune cell interactions identified by single-cell analysis, *Nat. Biotechnol.* 38 (2020) 970–979, <https://doi.org/10.1038/s41587-020-0602-4>.
- [69] K.M. Crosse, E.A. Monson, M.R. Beard, K.J. Helbig, Interferon-stimulated genes as enhancers of antiviral innate immune signaling, *J. Innate Immun.* 10 (2018) 85–93, <https://doi.org/10.1159/000484258>.
- [70] W. Wang, L. Xu, J. Su, M.P. Peppelenbosch, Q. Pan, Transcriptional regulation of antiviral interferon-stimulated genes, *Trends Microbiol.* 25 (2017) 573–584, <https://doi.org/10.1016/j.tim.2017.01.001>.
- [71] T.R. Rodrigues Prestes, N.P. Rocha, A.S. Miranda, A.L. Teixeira, E.S.A.C. Simoes, The anti-inflammatory potential of ACE2/angiotensin-(1-7)/mas receptor Axis: evidence from basic and clinical research, *Curr. Drug Targets* 18 (2017) 1301–1313, <https://doi.org/10.2174/1389450117666160727142401>.
- [72] P. Verdecchia, C. Cavallini, A. Spanevello, F. Angelini, The pivotal link between ACE2 deficiency and SARS-CoV-2 infection, *Eur. J. Intern. Med.* 76 (2020) 14–20, <https://doi.org/10.1016/j.ejim.2020.04.037>.
- [73] A.R. Fehr, R. Channappanavar, G. Jankevicius, C. Fett, J. Zhao, J. Athmer, et al., The conserved coronavirus macrodomain promotes virulence and suppresses the innate immune response during severe acute respiratory syndrome coronavirus infection, *mBio* 7 (2016), <https://doi.org/10.1128/mbio.01721-01716> doi: 10.1128/mbio.01721-16.
- [74] K. Sena, K. Furue, F. Setoguchi, K. Noguchi, Altered expression of SARS-CoV-2 entry and processing genes by Porphyromonas gingivalis-derived lipopolysaccharide, inflammatory cytokines and prostaglandin E2 in human gingival fibroblasts, *Arch. Oral Biol.* 129 (2021) 105201, <https://doi.org/10.1016/j.archoralbio.2021.105201>.
- [75] Y. Takahashi, N. Watanabe, N. Kamio, S. Yokoe, R. Suzuki, S. Sato, et al., Expression of the SARS-CoV-2 receptor ACE2 and proinflammatory cytokines induced by the periodontopathic bacterium Fusobacterium nucleatum in human respiratory epithelial cells, *Int. J. Mol. Sci.* 22 (2021) 1352.
- [76] N. Marouf, W. Cai, K.N. Said, H. Daas, H. Diab, V.R. Chinta, et al., Association between periodontitis and severity of COVID-19 infection: a case-control study, *J. Clin. Periodontol.* 48 (2021) 483–491, <https://doi.org/10.1111/jcpe.13435>.
- [77] J. Geng, L. Chen, Y. Yuan, K. Wang, Y. Wang, C. Qin, et al., CD147 antibody specifically and effectively inhibits infection and cytokine storm of SARS-CoV-2 and its variants delta, alpha, beta, and gamma, *Signal Transduct. Targeted Ther.* 6 (2021) 347, <https://doi.org/10.1038/s41392-021-00760-8>.
- [78] H. Ulrich, M.M. Pillat, CD147 as a target for COVID-19 treatment: suggested effects of azithromycin and stem cell engagement, *Stem Cell Reviews and Reports* 16 (2020) 434–440, <https://doi.org/10.1007/s12015-020-09976-7>.

- [79] E. Gkogkou, G. Barnasas, K. Vougas, I.P. Trougakos, Expression profiling meta-analysis of ACE2 and TMPRSS2, the putative anti-inflammatory receptor and priming protease of SARS-CoV-2 in human cells, and identification of putative modulators, *Redox Biol.* 36 (2020) 101615, <https://doi.org/10.1016/j.redox.2020.101615>.
- [80] H. Wang, Q. Yang, X. Liu, Z. Xu, M. Shao, D. Li, et al., Structure-based discovery of dual pathway inhibitors for SARS-CoV-2 entry, *Nat. Commun.* 14 (2023) 7574, <https://doi.org/10.1038/s41467-023-42527-5>.
- [81] M.V. Mateos-Moreno, A. Mira, V. Ausina-Márquez, M.D. Ferrer, Oral antiseptics against coronavirus: in-vitro and clinical evidence, *J. Hosp. Infect.* 113 (2021) 30–43, <https://doi.org/10.1016/j.jhin.2021.04.004>.
- [82] L. Martínez Lamas, P. Diz Dios, M.T. Pérez Rodríguez, V. Del Campo Pérez, J.J. Cabrera Alvargonzalez, A.M. López Domínguez, et al., Is povidone iodine mouthwash effective against SARS-CoV-2? First in vivo tests, *Oral Dis.* 28 (2022) 908–911, <https://doi.org/10.1111/odi.13526>.
- [83] K.B. Mar, N.R. Rinkenberger, I.N. Boys, J.L. Eitson, M.B. McDougal, R.B. Richardson, et al., LY6E mediates an evolutionarily conserved enhancement of virus infection by targeting a late entry step, *Nat. Commun.* 9 (2018) 3603, <https://doi.org/10.1038/s41467-018-06000-y>.
- [84] J.L. Tenthorey, M. Emerman, H.S. Malik, Evolutionary landscapes of host-virus arms races, *Annu. Rev. Immunol.* 40 (2022) 271–294, <https://doi.org/10.1146/annurev-immunol-072621-084422>.
- [85] X. Zhao, F. Guo, F. Liu, A. Cuconati, J. Chang, T.M. Block, et al., Interferon induction of IFITM proteins promotes infection by human coronavirus OC43, *Proc. Natl. Acad. Sci. USA* 111 (2014) 6756–6761, <https://doi.org/10.1073/pnas.1320856111>.
- [86] X. Zhao, M. Sehgal, Z. Hou, J. Cheng, S. Shu, S. Wu, et al., Identification of residues controlling restriction versus enhancing activities of IFITM proteins on entry of human coronaviruses, *J. Virol.* 92 (2018) e01535-01517, <https://doi.org/10.1128/JVI.01535-17>.
- [87] J. Yu, C. Liang, S.-L. Liu, Interferon-inducible LY6E protein promotes HIV-1 infection, *J. Biol. Chem.* 292 (2017) 4674–4685, <https://doi.org/10.1074/jbc.M116.755819>.
- [88] G. Shi, A.D. Kenney, E. Kudryashova, A. Zani, L. Zhang, K.K. Lai, et al., Opposing activities of IFITM proteins in SARS-CoV-2 infection, *EMBO J.* 40 (2021) e106501, <https://doi.org/10.15252/embj.2020106501>.
- [89] S.-M. Wang, K.-J. Huang, C.-T. Wang, Severe acute respiratory syndrome coronavirus spike protein counteracts BST2-mediated restriction of virus-like particle release, *J. Med. Virol.* 91 (2019) 1743–1750, <https://doi.org/10.1002/jmv.25518>.
- [90] L.-Y.R. Wong, P.-Y. Lui, D.-Y. Jin, A molecular arms race between host innate antiviral response and emerging human coronaviruses, *Virol. Sin.* 31 (2016) 12–23, <https://doi.org/10.1007/s12250-015-3683-3>.
- [91] M.E. Doyle, A. Appleton, Q.-R. Liu, Q. Yao, C.H. Mazucanti, J.M. Egan, Human type II taste cells express angiotensin-converting enzyme 2 and are infected by severe acute respiratory syndrome coronavirus 2 (SARS-CoV-2), *Am. J. Pathol.* 191 (2021) 1511–1519, <https://doi.org/10.1016/j.ajpath.2021.05.010>.